EUROPEAN ORGANIZATION FOR NUCLEAR RESEARCH (CERN)

FERMILAB-PUB-12-700-CMS

CERN-PH-EP/2012-077
2013/01/25

CMS-EXO-11-006

Search for anomalous $t\bar{t}$ production in the highly-boosted all-hadronic final state

The CMS Collaboration*

Abstract

A search is presented for a massive particle, generically referred to as a Z', decaying into a $t\bar{t}$ pair. The search focuses on Z' resonances that are sufficiently massive to produce highly Lorentz-boosted top quarks, which yield collimated decay products that are partially or fully merged into single jets. The analysis uses new methods to analyze jet substructure, providing suppression of the non-top multijet backgrounds. The analysis is based on a data sample of proton-proton collisions at a center-of-mass energy of 7 TeV, corresponding to an integrated luminosity of $5\,\text{fb}^{-1}$. Upper limits in the range of 1 pb are set on the product of the production cross section and branching fraction for a topcolor Z' modeled for several widths, as well as for a Randall–Sundrum Kaluza–Klein gluon. In addition, the results constrain any enhancement in $t\bar{t}$ production beyond expectations of the standard model for $t\bar{t}$ invariant mass larger than 1 TeV/c^2.

Submitted to the Journal of High Energy Physics

*See Appendix A for the list of collaboration members

1 Introduction

Among scenarios for physics beyond the standard model (SM) are possibilities of new gauge interactions with large couplings to third-generation quarks [1–11]. These interactions predict new massive states, generically referred to as Z' bosons, that can decay into $t\bar{t}$ pairs. Typical examples are the topcolor Z' described in Refs. [4–6], and the Randall–Sundrum Kaluza–Klein (KK) gluons of Ref. [12]. Other models [13–16] have recently been proposed to resolve the discrepancy in the forward-backward asymmetry in $t\bar{t}$ production reported at the Tevatron [17–21]. Model-independent studies of the implications of a large forward-backward asymmetry suggest that a strong enhancement of the production cross section for $t\bar{t}$ pairs would be expected at the Large Hadron Collider (LHC) for invariant masses $m_{t\bar{t}} > 1\,\text{TeV}/c^2$, if the observed discrepancy with the predictions of the standard model (SM) is due to new physics at some large mass scale [22, 23]. Searches for new physics in top-pair production have been performed at the Tevatron [24–26], and provide the most stringent lower limits on the mass ($m_{Z'}$) of narrow-width ($\Gamma_{Z'}$) resonances, e.g. excluding a topcolor $t\bar{t}$ resonance with $\Gamma_{Z'}/m_{Z'} = 1.2\%$ for masses below $\approx 0.8\,\text{TeV}/c^2$.

In this Letter, several models of resonant $t\bar{t}$ production are considered, including a Z' resonance with a narrow width of 1% of the mass, a Z' resonance with a moderate width of 10% of the mass, as well as broader KK gluon (g') states [12]. An enhancement over $t\bar{t}$ continuum production at large $t\bar{t}$ invariant masses is also considered.

This study examines decays of produced $t\bar{t}$ pairs in the all-hadronic channel, taking advantage of the large (46%) branching fraction of $t\bar{t} \to W^+bW^-\bar{b} \to 6$ quarks, and focuses on final states with $m_{t\bar{t}} > 1\,\text{TeV}/c^2$. For lower masses, the background from quantum-chromodynamic (QCD) production of non-top multijet events makes the search prohibitively difficult in this channel. At high $m_{t\bar{t}}$, using new techniques in jet reconstruction to identify jet substructure [27–31], it is possible to study highly boosted top quarks ($E/m_t c^2 > 2$, where E and m_t are the energy and mass of the top quark). The decay products of these highly boosted top quarks are collimated, and are partially or fully merged into single jets with several separate subjets corresponding to the final-state quarks (one from the bottom quark, and two light-flavor quarks from the W decay). The data sample corresponds to an integrated luminosity of $5\,\text{fb}^{-1}$ collected by the Compact Muon Solenoid (CMS) experiment [32] in proton-proton collisions at a center-of-mass energy of 7 TeV at the LHC.

In the following Letter, Sec. 2 describes the CMS detector and the event reconstruction. Section 3 explains the strategy for the analysis and the derivation of the efficiency and misidentification probability of the substructure tools that were used. Section 4 gives the systematic uncertainties in the analysis. Section 5 describes the statistical methodology used. Section 6 presents a summary of the results.

2 CMS detector, event samples, and preselection

The CMS detector is a general-purpose detector that uses a silicon tracker, as well as finely segmented lead-tungstate crystal electromagnetic (ECAL) and brass/scintillator hadronic (HCAL) calorimeters. These subdetectors have full azimuthal coverage and are contained within the bore of a superconducting solenoid that provides a 3.8 T axial magnetic field. The CMS detector uses a polar coordinate system with the polar angle θ defined relative to the direction (z) of the counterclockwise proton beam. The pseudorapidity η is defined as $\eta = -\ln\tan(\theta/2)$, which agrees with the rapidity $y = \frac{1}{2}\ln\frac{E+p_z c}{E-p_z c}$ for objects of negligible mass, where E is the energy and p_z is the longitudinal momentum of the particle. Charged particles are reconstructed

in the tracker for $|\eta| < 2.5$. The surrounding ECAL and HCAL provide coverage for photon, electron, and jet reconstruction for $|\eta| < 3$. The CMS detector also has extensive forward calorimetry that is not used in this analysis. Muons are measured in gas-ionization detectors embedded in the steel return yoke outside the solenoid.

Events were selected with an online trigger system, with decisions based on the transverse momentum (p_T) of a single jet measured in the calorimeters. The instantaneous luminosity increased with time, hence two thresholds were used for different running periods. Most of the data were collected with a threshold of jet $p_T > 300\,\text{GeV}/c$, and the rest with a threshold of $240\,\text{GeV}/c$. Offline, one jet is required to satisfy $p_T > 350\,\text{GeV}/c$.

There are several Monte Carlo (MC) simulated samples in the analysis. The continuum SM $\bar{t}t$ background is simulated with the MADEVENT/MADGRAPH 4.4.12 [33] and PYTHIA 6.4.22 [34] event generators. The MADGRAPH generator is also used to model generic high-mass resonances decaying to SM top pairs. In particular, a model is implemented with a Z′ that has SM-like fermion couplings and mass between 1 and 3 TeV/c^2. However, in the MC generation of the Z′, only decays to $\bar{t}t$ are simulated. The width of the resonance is set to 1% and 10% of $m_{Z'}$, so as to check the predictions for a narrow and a moderate resonance width, respectively. Here, the 10% width is comparable to the detector resolution. The PYTHIA 8.145 event generator [35] is used to generate Randall–Sundrum KK gluons with masses $m_{g'} = 1$, 1.5, 2, and 3 TeV/c^2, and widths of $\approx 0.2 m_{g'}$. These Randall–Sundrum gluons have branching fractions to $\bar{t}t$ pairs of 0.93, 0.92, 0.90, and 0.87, respectively. PYTHIA6 is also used to generate non-top multijet events for background studies, cross-checks, and for calculating correction factors. The CTEQ6L [36] parton distribution functions (PDF) are used in the simulation. The detector response is simulated using the CMS detector simulation based on GEANT4 [37].

Events are reconstructed using the particle-flow algorithm [38], which identifies all reconstructed observable particles (muons, electrons, photons, charged and neutral hadrons) in an event by combining information from all subdetectors. Event selection begins with removal of beam background by requiring that events with at least 10 tracks have at least 25% of the tracks satisfying high-purity tracking requirements [39]. The events must have a well-reconstructed primary vertex, and only charged particles identified as being consistent with the highest Σp_T^2 interaction vertex are considered, reducing the effect of multiple interactions per beam crossing (pile-up) by $\approx 60\%$.

The selected particles, after removal of charged hadrons from pile-up and isolated leptons, are clustered into jets using the Cambridge-Aachen (CA) algorithm with a distance parameter of $R = 0.8$ in η-ϕ space, where ϕ is the azimuthal angle [40, 41], as implemented in the FASTJET software package version 2.4.2 [42, 43]. The CA algorithm sequentially merges into single objects, by four-vector addition, the pairs of particle clusters that are closest in the distance measure $d_{ij} = \Delta R_{ij}^2 / R^2$, where $\Delta R_{ij} = \sqrt{(\Delta\eta)^2 + (\Delta\phi)^2}$ and $R = 0.8$, until the minimum is less than or equal to the so-called beam distance d_{iB}, which equals unity in the CA algorithm. More generally these distance measures are equal to $d_{ij} = \min(p_{T_i}^{2n}, p_{T_j}^{2n}) \Delta R_{ij}^2 / R^2$ and $d_{iB} = p_{T_i}^{2n}$. In the more common cases of the k_T and anti-k_T algorithms [44], $n = 1$ and $n = -1$, respectively, however for the CA algorithm $n = 0$, and hence only angular information is used in the clustering. When the beam distance for particle cluster i is smaller than all of the other d_{ij}, particle cluster i is identified as a jet and the clustering proceeds for the remaining particles in the event. Jet energy scale corrections are applied as documented in Ref. [45]. All jets are required to satisfy jet-quality criteria [38], as well as $|y| < 2.5$. The rapidity is used in this case because the jets acquire a finite mass as part of the imposed jet-quality criteria.

3 Analysis method

The analysis is designed for cases in which the $\mathrm{t\bar{t}}$ system has sufficient energy for the decay products of each top quark to be emitted into a single hemisphere, implying that $E/m_{\mathrm{t}}c^2 > 2$. As a consequence, the top quarks can be either partially merged when only the W decay products are merged into a single jet, or fully merged when all top decay products are merged into a single jet. Thus, this analysis becomes inefficient for low masses, and upper limits are not evaluated for Z' masses below $1\,\mathrm{TeV}/c^2$.

The largest background in this search is the non-top multijet (NTMJ) background. This is highly suppressed by requirements on the jet mass and substructure. The remaining NTMJ background is estimated by computing the probability for non-top jets to pass the top-jet selections (misidentification probability) in control regions of the data. These control regions are constructed by inverting substructure selections while keeping mass selections fixed. This mistagging probability is then applied to the signal region to estimate the contribution from the NTMJ background.

In this section, the jet topologies in the analysis are defined in Sec. 3.1, the signal estimate is described in Sec. 3.2, and the background estimate is shown in Sec. 3.3. Finally, the results of the event selection and the background estimate are presented in Sec. 3.4.

3.1 Analysis of jet topologies

The events are classified into two categories, depending on the number of final-state jets that appear in each hemisphere. The 1+1 channel comprises dijet events in which each jet corresponds to a fully merged top-quark candidate, denoted as a Type-1 top-quark candidate. The 1+2 channel comprises trijet events that fail the 1+1 criteria, with a Type-1 top-quark candidate in one hemisphere, and at least two jets in the other, one being a jet from a b quark (although no identification algorithms are applied) and the other a merged jet from a W. These two separate jets define a Type-2 top-quark candidate in the 1+2 channel. Further channels, such as 2+2, which would correspond to two Type-2 top quarks, are not considered in this analysis. The 1+1 and 1+2 selections are now discussed in detail.

The 1+1 events are required to have at least two Type-1 top-quark candidates, each reconstructed with $p_{\mathrm{T}} > 350\,\mathrm{GeV}/c$. Both candidates are tagged by a top-tagging algorithm [27, 28] to define merged top jets. In the case of more than two top-tagged jets, the two top-tagged jets with the highest p_{T} are considered. The top-tagging algorithm is based on the decomposition of a jet into subjets, by reversing the final steps of the CA jet-clustering sequence. In this decomposition, particles that have small p_{T} or are at large angles relative to the parent cluster are ignored. At least three subjets are required in each jet. While the subjets of generic jets tend to be close together, and one of them often dominates the jet energy because of gluon emission in the final state, the decay products of the top quark share the jet energy more equally and emerge at wider angles. The mass of the summed four-vector of the constituents of the hard jet must be consistent with the mass of a top quark $m_{\mathrm{t}} \approx 175\,\mathrm{GeV}/c^2$ ($140 < m_{\mathrm{jet}} < 250\,\mathrm{GeV}/c^2$, where the values chosen are optimized through MC simulation). Figure 1a shows the expected jet mass for the Z' signal from MC as a dotted histogram, and the expected jet mass for the NTMJ background from MC as a solid yellow histogram. As expected, the Z' signal has a peak at the top mass corresponding to fully merged top jets, and has a shoulder at the W mass corresponding to partially merged top jets. The minimum pairwise invariant mass of the three subjets of highest p_{T} is required to be $> 50\,\mathrm{GeV}/c^2$, because the combination with the minimum pairwise mass often ($> 60\%$) consists of the jet remnants from the W decay.

The 1+2 events are required to have exactly one hemisphere containing a top-tagged Type-1 candidate with $p_T > 350\,\text{GeV}/c$. That is, only events that fail the 1+1 criteria are considered for the 1+2 selection. In the hemisphere opposite the top-tagged Type-1 candidate, there must be at least two jets, one identified as a W-jet candidate, with $p_T > 200\,\text{GeV}/c$, and another jet from a b quark (although no identification algorithm is used) with $p_T > 30\,\text{GeV}/c$. The W jet is required to be tagged by a W-tagging algorithm, based on the jet pruning technique [29, 30]. The W-tagging algorithm requires two subjets, a total jet mass consistent with the mass of the W boson $m_W = 80.4\,\text{GeV}/c^2$ ($60 < m_{\text{jet}} < 100\,\text{GeV}/c^2$), and an acceptable "mass-drop" parameter μ of the final subjets relative to the hard jet [31]. The mass-drop μ is defined as the ratio of the mass of the more massive subjet m_1 to the mass of the complete jet m_{jet}, and is required to be smaller than 40% ($m_1/m_{\text{jet}} \equiv \mu < 0.4$). This selection helps to discriminate against generic jets, which usually have larger μ values. The W-jet and b-jet candidates combine to form the Type-2 top-quark candidate, whose mass must be consistent with that of the top quark ($140 < m_{\text{jet}} < 250\,\text{GeV}/c^2$, where the values chosen are optimized using MC simulation). When there are more than two jets in the Type-2 hemisphere, the b-quark candidate is taken as the one closest to the W-tagged jet in η-ϕ space.

The jet-pruning technique used to select W jets removes a portion of the jet, which is not accounted by the ordinary jet energy scale corrections. The jet corrections used in this analysis are derived from unpruned jets, and the impact on pruned jets is therefore investigated using a dijet MC sample. In particular, the p_T of reconstructed pruned jets are compared to the p_T of matched generator-level particle jets, that also underwent the pruning procedure, and the difference of 2–3% observed in absolute response suggests a systematic uncertainty in the jet energy from this source. An uncorrelated 3% uncertainty is therefore added to the uncertainties for standard jet energy corrections. This uncertainty is applied for both the top-tagging and jet-pruning algorithms, and is added in quadrature to the general jet energy scale corrections of Ref. [45], which are $\approx$ 2–4%, depending on p_T and rapidity.

3.2 Signal efficiency

For both the Z' signal and the (subdominant) $t\bar{t}$ background, the efficiencies of the analysis selection are estimated from Monte Carlo simulation, with scale factors to account for measured differences with respect to the data. Figure 1b shows the efficiency for tagging a true top jet as a function of p_T. Above $\approx 500\,\text{GeV}/c$, the efficiency plateaus between 50–60%.

Three scale factors are applied to the efficiency. The first scale factor is used to correct for the trigger in simulated signal events. Its value is equal to the trigger efficiency: it rises from $\approx$ 75% (60%) for 1+1 (1+2) events at $m_{t\bar{t}} = 1.0\,\text{TeV}/c^2$ and becomes fully efficient for $m_{t\bar{t}} > 1.5\,\text{TeV}/c^2$. The value of the trigger efficiency is estimated per jet on a sample of simulated NTMJ events passing the top-quark candidate selections, it is then applied to simulated signal events. The systematic uncertainty is assigned to be 50% of the trigger inefficiency from MC. The difference between the measured trigger efficiency in data and MC is roughly in this range, but suffers from large statistical uncertainties. The second scale factor is used to correct for any differences in jet-energy scale for the subjets and for the full jets. This is referred to as the subjet jet-energy scale factor. The third scale factor is used to correct for the impact of any differences between data and MC in efficiencies for finding jets with substructure. This is referred to as the subjet selection-efficiency scale factor. The derivation of the second and third scale factors is now discussed in detail.

These second two scale factors are both determined in a control sample comprising events with a single muon (referred to as the muon control sample), usually from the decay of $t \to Wb$,

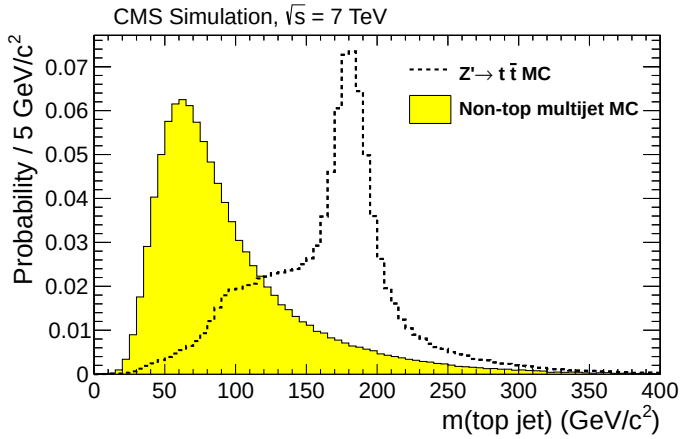

(a)

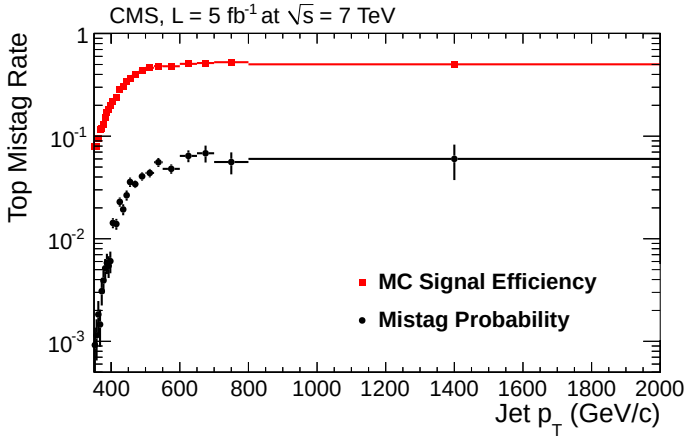

(b)

Figure 1: (a) The simulated jet mass for NTMJ MC (light yellow histogram) and Z′ MC (open histogram). (b) The type-1 per-jet top-tagging efficiency for Z′ MC events is shown as red squares with error bars (see Sec. 3.2), and the type-1 per-jet mistag probability for top tagging measured in data is shown as black circles with error bars (see Sec. 3.3), both as a function of jet p_{T}.

with $W \to \mu\nu$, and at least two jets. The event selection is nearly identical to that in Ref. [46], except for larger p_T requirements for the jets. The leading jet is required to satisfy $p_T > 200$ GeV/c, and the sub-leading jet is required to satisfy $p_T > 30$ GeV/c. Due to a small number of fully-merged (Type-1) top jets in this sample, it is not possible to construct a sufficiently large number of true Type-1 top jets. Instead, the characterization of jets with substructure is studied with moderately-boosted $t\bar{t}$ events where there is a large fraction of partially-merged (Type-2) top-quark candidates and the W-jets within them.

The events in the muon control sample used to study W-tagging are dominated by $t\bar{t}$ decays, and the leading-jet p_T requirement (> 200 GeV/c) favors the topology in which the two top quarks are produced back-to-back, thereby facilitating jet merging on the side of the "hadronic" top quark, containing jets from $t \to Wb \to q\bar{q}'b$. In the other hemisphere, these events contain one isolated muon, consistent with originating from the primary collision vertex, with $p_T > 45\,\text{GeV}/c$ and $|\eta| < 2.1$. Events are rejected if they contain other isolated electrons or muons within $|\eta| < 2.1$ with $p_T > 15\,\text{GeV}/c$ or $p_T > 10\,\text{GeV}/c$, respectively. The remaining events are then required to have ≥ 2 jets with $p_T > 30\,\text{GeV}/c$, and at least one jet with $p_T > 200\,\text{GeV}/c$. Unlike the all-hadronic channel discussed in this Letter, in the muon control sample, there are two well-separated jets originating from b quarks, so in order to enhance the $t\bar{t}$ fraction of this control region, the events are required to contain at least one jet tagged with a secondary-vertex b-tagging algorithm [47], also used in Ref. [46]. The b-tagging algorithm combines at least two tracks into at least one secondary vertex, and forms a discriminating variable based on the three-dimensional decay length of the vertex.

The subjet jet-energy scale factor is estimated by extracting a W mass peak in the muon control sample, and comparing the peaks in data and MC. The mass distribution of the jet of largest mass in the hadronic hemisphere is shown in Fig. 2a.

In this figure, the MC $t\bar{t}$ contribution is normalized to the approximate next-to-next-to-leading-order (NNLO) cross section for inclusive $t\bar{t}$ production of 163 pb [48–50]. The non-W mulitjet component is based on sidebands in data that have the muon isolation criterion reversed. The contributing spectrum is normalized through a fit to the missing transverse energy. The stringent criteria of this analysis provide very few W+jets events that pass the required selections. This distribution is therefore taken to be the same as that of the generic non-W multijet background. This is acceptable because the mass structure within the candidate top-quark jets are very similar in these two samples, and the sideband data has many more events that pass the selection criteria. The W+jets contribution is normalized to the inclusive W production cross section of $\sigma_{W\to\ell+\nu} = 31.3 \pm 1.6$ nb computed at NNLO with FEWZ [51]. A fit of the sum of two Gaussian functional forms to data is given by the solid line, and a similar fit to the simulated events is shown as a dashed line. The centers of the main Gaussian distributions in data and MC are $m_W^{\text{DATA}} = 83.0 \pm 0.7\,\text{GeV}/c^2$ and $m_W^{\text{MC}} = 82.5 \pm 0.3\,\text{GeV}/c^2$, respectively. The subjet jet-energy scale factor for W jets is determined by taking the ratio of these two values, and equals 1.01 ± 0.01, including statistical uncertainty only.

The subjet selection-efficiency scale factor is estimated by comparing the observed selection efficiency in the muon control sample in data and MC. The ratio of the number of events in the W mass window ($60 < m_{\text{jet}} < 100$ GeV/c^2) in Fig. 2a, after W tagging, to the number of events in the muon control sample, defines the W selection efficiency within the mass window. For data and MC the values are $\epsilon_{m_W}^{\text{DATA}} = 0.49 \pm 0.01$ and $\epsilon_{m_W}^{\text{MC}} = 0.50 \pm 0.01$, respectively. Similarly, the mass-drop selection is checked in data and Monte Carlo, following the W-mass window selection, and a similar efficiency is extracted, with the observed values being $\epsilon_\mu^{\text{DATA}} = 0.64 \pm 0.01$ and $\epsilon_\mu^{\text{MC}} = 0.64 \pm 0.01$. Combining efficiencies of the mass-drop and mass selections,

the subjet selection-efficiency scale factor, to be applied to the MC to obtain the same efficiency as in data, is determined to be 0.97 ± 0.03. The same scale factor and uncertainty are assumed for Type-1 jets, which is consistent with results from the statistics-limited control sample of muon events that contain Type-1 jets. As two top-quark tags are required in each event, the correction for both 1+1 and 1+2 events is the square of the single-tag scale factor, yielding 0.94 ± 0.06.

The Type-1 jet selection cannot be checked at the same level of precision as the W-jet selection because of the small number of Type-1 jets in the muon control sample. However, the Type-2 top-quark candidate selection can be tested in the muon control sample, as shown in Fig. 2b. The same procedure is used to construct these Type-2 top-quark candidates as in the 1+2 selection, including the W-mass and mass-drop selections. Within the statistical uncertainty, good agreement is observed in the data and simulation. Since the selection of Type-2 top-quark candidates considers a boosted three-body decay as well as a W tag, the agreement between the characteristics of candidates in data and in MC provides further confidence for the assumption that the scale factor for the efficiency of W-tagging is appropriate for three-body decays such as the Type-1 top-quark system.

To check the dependability of our assumption, namely that the data-to-MC scale factors are the same for the muon control sample as for the Z' signal, the scale factor is measured in a control sample using more stringent kinematic requirements to select a part of phase space similar to that of a Z' signal with $m \sim 1\,\text{TeV}/c^2$. The b-tagging requirement is dropped in order to collect more $\bar{t}t$ events. Also, to capture the kinematics of the background, instead of using the distribution for W+jets from the sidebands in data without isolated muon candidates, as is done in the fit to the W mass, the distribution for W+jets is taken instead from the W+jets MC.

In all samples with large p_T thresholds, the data-to-MC scale factor is found to be consistent with the measured value of 0.97 ± 0.03. The selection that provides sideband regions most similar in kinematics to that of the signal region is a requirement that the Type-2 top candidate satisfy $p_T > 400$ GeV/c. Fig. 3a shows the p_T distribution for the Type-2 candidates in the muon control sample, and Fig. 3b shows the p_T of the W-jet within the Type-2 top-quark candidate, as defined by the jet of largest mass in the event. Arbitrarily normalized distributions for a Z' signal with $m = 1$ TeV/c^2 are overlaid for comparison. For completeness, Figs. 4a and 4b show plots identical to Figs. 2a and 2b, but with selections that require Type-2 top-quark candidates with $p_T > 400$ GeV/c. The scale factor extracted from this higher-p_T subsample is 0.99 ± 0.11, which is consistent with the quoted data-to-MC scale factor of 0.97 ± 0.03.

3.3 Background estimate

Since this analysis focuses on signatures with high-p_T jets, the main backgrounds expected are from SM non-top multijet production and $\bar{t}t$ production. The background from NTMJ production is estimated from sidebands in the data as described below. For the Z' masses considered in this analysis, the irreducible SM $\bar{t}t$ component is significantly smaller than the NTMJ background contribution, and is therefore estimated from MC simulation using the same correction factors as found for the Z' MC described in Sec. 3.2. It is normalized to the approximate NNLO cross section described in Sec. 3.2.

In both 1+1 and 1+2 channels, estimates of the dominant NTMJ background are obtained from data as follows. First, the probability is estimated for mistaking a non-top jet as a top-quark jet through the top-tagging algorithm. This procedure defines the mistag probability (P_m). Higher momentum jets have a larger probability to radiate gluons, and as the jet p_T increases, they are more likely to have top-like substructure and thereby satisfy a top tag [52]. The mistag

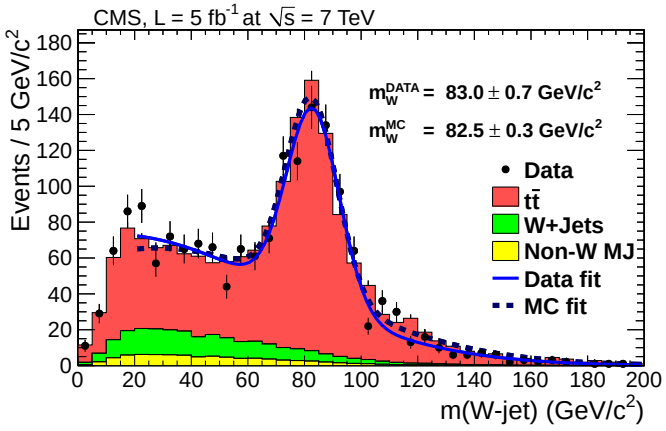

(a)

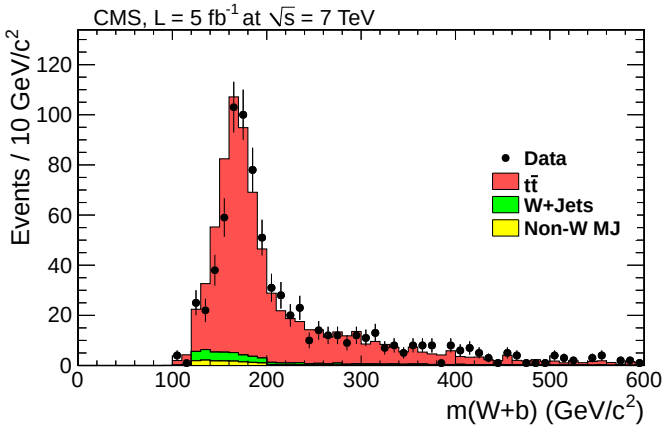

(b)

Figure 2: (a) The mass of the highest-mass jet (W-jet), and (b) the mass of the Type-2 top candidate (W + b), in the hadronic hemisphere of moderately-boosted events in the muon control sample. The data are shown as points with error bars, the $t\bar{t}$ Monte Carlo events in dark red, the W+jets Monte Carlo events in lighter green, and non-W multijet (non-W MJ) backgrounds are shown in light yellow (see Ref. [46] for details of non-W MJ distribution derivation). The jet mass is fitted to a sum of two Gaussians in both data (solid line) and MC (dashed line), the latter of which lies directly behind the solid line for most of the region.

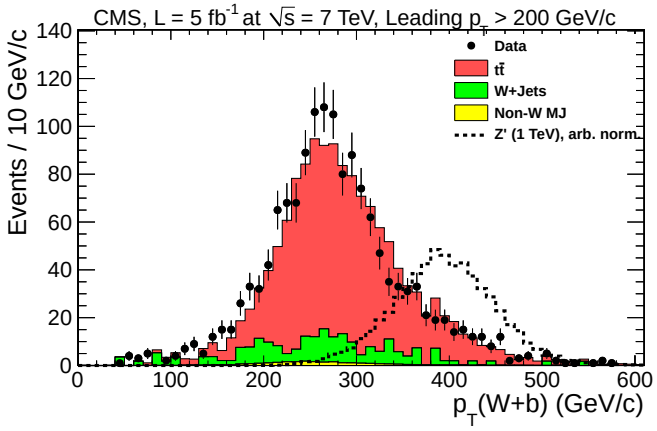

(a)

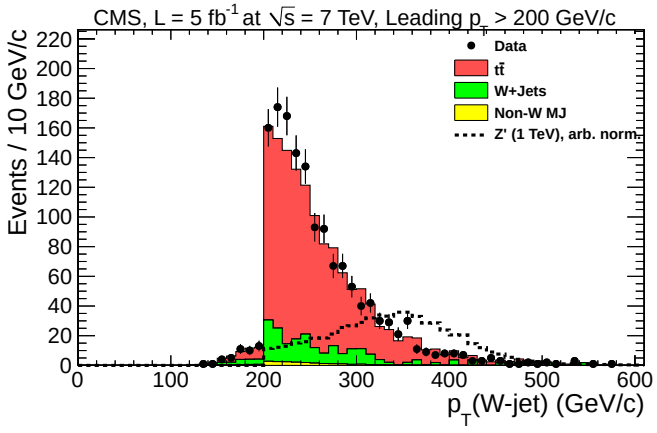

(b)

Figure 3: (a) p_{T} of the Type-2 top-quark candidate in the muon control sample. The color scheme is the same as in Figs. 2a and 2b. (b) p_{T} of the W-candidate from within the Type-2 top-quark candidate, after a selection on the jet mass of the highest-mass jet in the muon control sample. Overlaid on both (a) and (b) are the corresponding distributions from a Z' MC signal with $m = 1$ TeV/c^2 (with arbitrary normalization for visualization) to compare kinematics in the muon control region to the signal region.

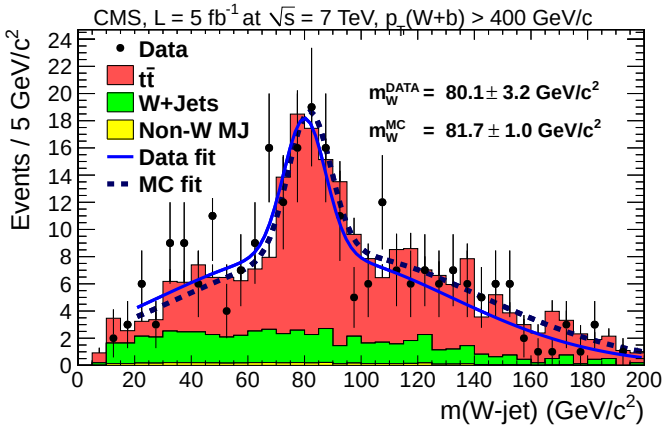

(a)

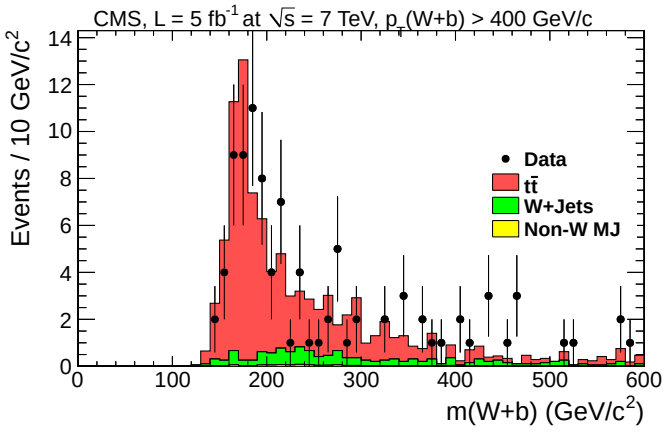

(b)

Figure 4: (a) The mass of the highest-mass jet (W-jet), and (b) the mass of the Type-2 top candidate (W + b), in the hadronic hemisphere of moderately-boosted events in the muon control sample. The Figure corresponds to Figs. 2a and 2b, except there is an additional requirement on the Type-2 top candidate p_{T} to be similar to the signal region. Figure 3a shows the distribution of the Type-2 top candidate p_{T}.

probability is therefore obtained as a function of total jet p_T, using the following procedure. Events with ≥ 3 jets are selected for the 1+2 topology, with the three leading jets in the event required to pass p_T thresholds of 350, 200, and 30 GeV/c, respectively, without any requirements placed on the jet mass of the Type-1 candidate. The mass of the W-boson candidate within the Type-2 candidate is required to fall within the W-boson mass window, and the invariant mass of the Type-2 candidate is required to fall within the top-quark mass window. However, the mass-drop requirement is inverted ($\mu > 0.4$) to define a signal-depleted sideband. The small contribution from the SM $\mathrm{t\bar{t}}$ continuum is subtracted using MC expectation, and the mistag probability $P_m(p_T)$ is defined by the fraction of Type-1 candidates that are top-tagged, as a function of their p_T. The resulting mistag probability appears in Fig. 1b.

Next, the 1+2 and 1+1 samples are defined using a loose selection: (i) in trijet events, two jets in one hemisphere are required to pass the Type-2 selection and (ii) in dijet events, one randomly-chosen jet is required to pass the Type-1 selection. In both cases, the other high-p_T jet in the event (the probe jet) is not required to be top-tagged. These samples are dominated by NTMJ events. For each event in the loose selection (i), the probability that the event would pass the full selection in the signal region (P^i_{NTMJ}) equals the mistag probability ($P_m(p_T)$), evaluated at the p_T of the probe jet in event i (p^i_T),

$$P^i_{\mathrm{NTMJ}} = P_m(p^i_T). \tag{1}$$

The total number of NTMJ events (N_{NTMJ}) is then equal to the sum of the weights from Eq. 1.

$$N_{\mathrm{NTMJ}} = \sum_{i=1}^{N_{\mathrm{loose}}} P^i_{\mathrm{NTMJ}} = \sum_{i=1}^{N_{\mathrm{loose}}} P_m(p^i_T), \tag{2}$$

where N_{loose} is the number of events passing the loose selection and the other quantities are defined above.

The ensemble of jets in the loose pretagged region have, on average, a lower jet mass than the jets in the signal region. Consequently, the $m_{\mathrm{t\bar{t}}}$ spectrum in this sideband is kinematically biased. To emulate the event kinematics of the signal region, the jet mass of the probe jet is ignored, and instead it is set to a value randomly drawn from the distribution of jet masses of probe jets from NTMJ MC events in the range 140 to 250 GeV/c^2.

This procedure is cross-checked on a NTMJ MC sample to ensure that the methodology achieves closure. In this cross-check, half of the events in the MC are used to derive a mistag probability using the above procedure, and then used to predict the expected number of tags for the remaining events, which is compared to the observed number of tags in these events. The observed and expected number of tags agree within statistical uncertainties.

Possible biases in the calibration procedure from the presence of a new Z′ have also been investigated in the analysis. For instance, a Z′ signal with $m_{Z'} = 3$ TeV/c^2 and a width of 30 GeV/c^2 contributes less than 1% to the events defined through the loose selection criteria as well as to the sideband regions used to determine the probability of mistagging jets.

The uncertainty on this procedure is taken as half the difference between the $m_{\mathrm{t\bar{t}}}$ distributions obtained using the modified and unmodified probe-jet masses. Two choices of alternative prior distributions for the probe-jet mass were investigated, the MC-based prior described above, and a flat prior. The systematic uncertainty estimated with the current method is slightly more conservative.

Table 1: The number of events observed in the loose selection (N_{loose}), which is used as input to compute the number of events predicted in the signal region for the mistagged NTMJ background (N_{NTMJ}). Both appear in Eq. 2 and are described in detail in Sec. 3.3. Figure 1b shows the value $P_{\text{m}}(p_{\text{T}})$ used in Eq. 2. For N_{NTMJ}, the first and second uncertainties are statistical and systematic, respectively.

	$m_{\text{t}\bar{\text{t}}}$ =0.9–1.1 TeV/c^2		$m_{\text{t}\bar{\text{t}}}$ =1.3–2.4 TeV/c^2	
	1+1	1+2	1+1	1+2
N_{loose}	22015	70545	18401	30253
N_{NTMJ}	$443 \pm 4 \pm 22$	$1239 \pm 6 \pm 31$	$741 \pm 6 \pm 30$	$817 \pm 6 \pm 36$

Table 2: Expected and observed number of events in two different $\text{t}\bar{\text{t}}$ mass windows for the 1+1 and 1+2 samples. The expected SM $\text{t}\bar{\text{t}}$ is taken from MC predictions, and the expected NTMJ background is derived in Table 1.

	$m_{\text{t}\bar{\text{t}}}$ =0.9–1.1 TeV/c^2		$m_{\text{t}\bar{\text{t}}}$ =1.3–2.4 TeV/c^2	
	1+1	1+2	1+1	1+2
Expected SM $\text{t}\bar{\text{t}}$ events	69 ± 36	110 ± 62	65 ± 42	24 ± 15
Expected non-top multijet events	443 ± 23	1239 ± 32	741 ± 32	817 ± 38
Total expected events	512 ± 43	1349 ± 70	806 ± 53	841 ± 41
Observed events	506	1383	809	841

Table 1 provides an estimate for the mistagged NTMJ background for two $\text{t}\bar{\text{t}}$ mass windows: 0.9–1.1 TeV/c^2 and 1.3–2.4 TeV/c^2. The first row corresponds to the number of events observed in the loose selection (N_{loose} from Eq. 2) to which the mistag probability is applied. The second row corresponds to the number of expected events from the mistagged NTMJ background in the signal region (N_{NTMJ} in Eq. 2). As can be observed in Table 1, the primary uncertainty on the NTMJ background is from the systematic uncertainty assigned to the procedure for modifying probe-jet masses.

3.4 Results of event selection

Observed $m_{\text{t}\bar{\text{t}}}$ distributions for 1+1 and 1+2 events in data are compared to the expected backgrounds in Fig. 5. The NTMJ background expectation determined from data is given by the yellow (light) filled histograms. The SM $\text{t}\bar{\text{t}}$ estimate is shown as red (dark) filled histograms, and the data are shown as solid black points. The hatched gray regions indicate the total uncertainty on the backgrounds. Figure 5 also shows for comparison the signal expectation from MC for several hypothetical Z′ signals with masses from 1 to 3 TeV/c^2 with a width of 1%, in the 1+1 and 1+2 samples, but with cross sections taken from the expected limits discussed in Sec. 5.1.

From Fig. 5, it is clear that the dominant background in this analysis is from NTMJ events rather than from SM $\text{t}\bar{\text{t}}$ production. The implementation of b-quark selections has not as yet been introduced to improve the sensitivity of this search, and must await an improvement in performance of b-tagging in merged top jets.

To demonstrate the components of the background estimate, Table 2 lists the number of events expected from background sources in the 1+1 and 1+2 channels, along with the observed number of events, for two $\text{t}\bar{\text{t}}$ mass windows: from 0.9–1.1 TeV/c^2, and 1.3–2.4 TeV/c^2. The systematic uncertainties on these values are now summarized in Sec. 4.

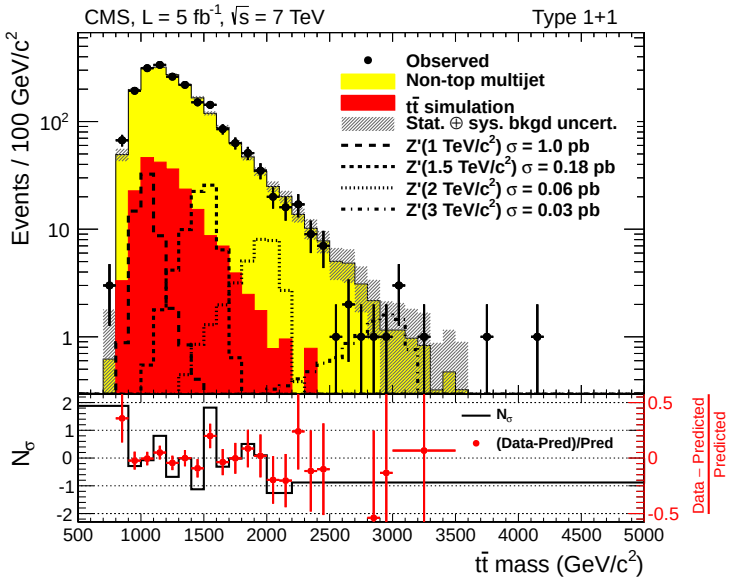

(a)

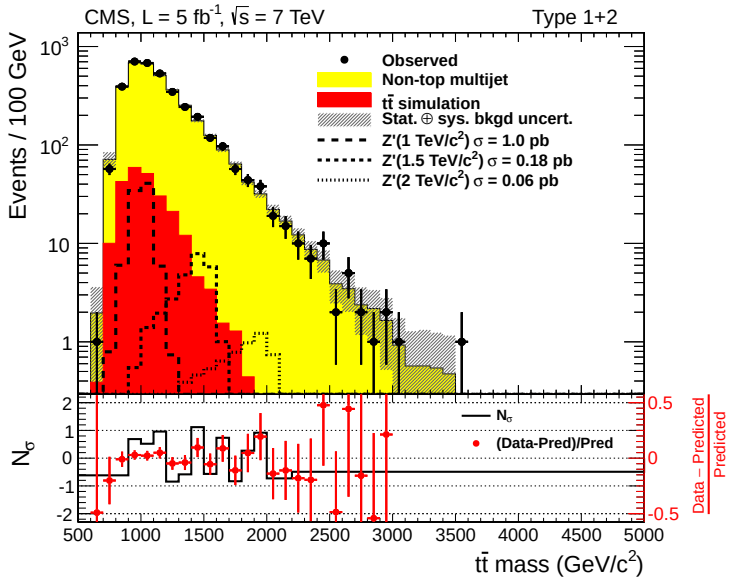

(b)

Figure 5: Results for (a) 1+1 and (b) 1+2 event selections and background estimates. The yellow (light) histograms are the non-top multijet (NTMJ) estimates from data, as described in the text, and the red (dark) histograms are the MC estimates from SM $t\bar{t}$ production. The black points are the data. The hatched gray boxes combine the statistical and systematic uncertainties on the total background. For comparison, expectations for some Z′ hypotheses are shown for the assumption of 1% resonance width, with cross sections taken from the expected limits discussed in Sec. 5.1. Also shown are the ratio of the fractional difference between the data and the prediction, shown in red circles, with the y-axis on the right of the plot, and the number of standard deviations (N_σ) of the observation from the prediction, shown as a black histogram with the y-axis on the left of the plot, where the binning is adjusted to have at least 20 events in each bin.

4 Systematic uncertainties

The sources of systematic uncertainty on the $t\bar{t}$ invariant mass spectrum fall into three categories: (i) the determination of the efficiency, (ii) the mistag probability, and (iii) the shape of the $t\bar{t}$ invariant-mass distribution. Several sources of systematic uncertainties can simultaneously affect these three categories, and in such cases, any changes in parameters have to be varied in a correlated way. The uncertainties on efficiency include uncertainties in the overall jet-energy scale for tagged jets ($\approx$ 2–4% from standard jet energy corrections, $\approx$ 3% from the application of the jet corrections to pruned jets, and $\approx$ 1% to account for the uncertainty on the determination of the W mass in data and MC, as described in Sec. 3.2), integrated luminosity (2.2%), subjet-selection efficiency ($\approx$ 6%, as described in Sec. 3.2), jet energy resolution ($<$ 1%), and jet angular resolution ($<$ 1%). The trigger uncertainty for 1+1 events is 13% for $m_{t\bar{t}} = 1\,\text{TeV}/c^2$, and $<$ 1% for $t\bar{t}$ masses above $1.5\,\text{TeV}/c^2$. The trigger uncertainty is larger for 1+2 events: 20% for $m_{t\bar{t}} = 1\,\text{TeV}/c^2$, and 3% for $m_{t\bar{t}} > 1.5\,\text{TeV}/c^2$, as described in Sec. 2. The impact of changes in parton distribution functions [53] is found to be negligible.

Similar uncertainties affect the $t\bar{t}$ continuum background and are estimated in the same manner. In addition, the large uncertainty on the renormalization and factorization scales (a factor of two) is found to have significant impact on SM $t\bar{t}$ production, resulting in a 50% variation in the yield, estimated from MC studies. This is reflected in the uncertainties on the number of $t\bar{t}$ events in Table 2. Table 3 provides a summary of this information.

Table 3: Summary of relative systematic uncertainties on signal efficiency for two $t\bar{t}$ mass windows. All values are in percent. The central value of the subjet selection scale factor is 0.94, it is the only scale factor that has a non-unit mean.

Source	Variation	$m_{t\bar{t}}$ =0.9–1.1 TeV/c^2		$m_{t\bar{t}}$ =1.3–2.4 TeV/c^2	
		1+1	1+2	1+1	1+2
MC Statistical		2.0	1.6	0.7	1.6
Trigger	See text	13	20	<1	3
Jet energy scale	$\approx \pm 5$	19	19	2	2
Subjet efficiency scale factor	$\pm$ 6	6	6	6	6
Luminosity	$\pm$ 2.2	2.2	2.2	2.2	2.2
Total		24	28	7	8

The uncertainties on the mistagged NTMJ background include the statistical uncertainty on the sample after loose selection, to which the mistag probability is applied; the statistical uncertainty on the mistag probability itself, ranging from $<$ 1% at $1\,\text{TeV}/c^2$ to $\approx$ 10% at $3\,\text{TeV}/c^2$ as seen in Fig. 1b; and the systematic uncertainty on the mistag probability application, as described in Sec. 3.3, which is in the range of 1 to 5% depending on the $t\bar{t}$ mass. The total background uncertainty is $\approx$ 5% for the low-mass region, dominated by the systematic uncertainty, and $\approx$ 100% for the high-mass region, dominated by statistical uncertainty associated with the sample after loose selection.

5 Statistical treatment

The main result of this analysis is the fit to data assuming a resonance hypothesis for the new physics, in which a likelihood is fit to the expected $t\bar{t}$ invariant mass distributions for signal and background. The second result corresponds to a counting of events relative to some generic model of an enhancement of the $t\bar{t}$ continuum assuming the SM efficiency for the additional contribution. These two results are discussed below.

5.1 Resonance analysis

The first analysis uses a resonant signal hypothesis to search for localized contributions to the $m_{\mathrm{t\bar{t}}}$ spectrum. A cross-check of the analysis is performed by counting the number of events in a mass range defined for each resonant mass value. Two such mass ranges are shown in Tables 1-3. In the main resonance analysis and the cross-check, the number of observed events, N_{obs}, is compared to the expectation N_{exp}, based on the production cross section $\sigma_{Z'}$, branching fraction $B(Z' \to \mathrm{t\bar{t}})$, signal reconstruction efficiency ϵ, integrated luminosity L, and the predicted number of background events N_B:

$$N_{exp} = \sigma_{Z'} \times B(Z' \to \mathrm{t\bar{t}}) \times \epsilon \times L + N_B. \tag{3}$$

The likelihood is computed using the Poisson probability to observe N_{obs}, given a mean of N_{exp}, with uncertain parameters L, ϵ, and N_B, all defined through log-normal priors based on their mean values and their uncertainties. The shapes and normalizations of signal and background distributions are varied within their systematic uncertainties until the likelihood is maximized. This procedure effectively integrates over the parameters describing the systematic uncertainties, thereby reducing their impact.

The upper limits at 95% confidence level (CL) on the product of the Z′ production cross section and the branching fraction to the $\mathrm{t\bar{t}}$ final state are extracted for the combination of the 1+1 and 1+2 $\mathrm{t\bar{t}}$ mass spectra, as a function of $m_{Z'}$ in a range from 1 to 3 TeV/c^2 with a 0.1 TeV/c^2 increment. A CL_S method [54–56] is used to extract the 95% CL upper limits, with the posterior based on a Poisson model for each bin of the $m_{\mathrm{t\bar{t}}}$ distribution.

Figure 6 shows the observed and expected upper limits for: (a) a Z′ hypothesis with $\Gamma_{Z'}/m_{Z'} = 1\%$, (b) a Z′ hypothesis with $\Gamma_{Z'}/m_{Z'} = 10\%$, and (c) a Randall–Sundrum Kaluza–Klein gluon hypothesis. Also shown are the theoretical predictions for several models to compare to the observed and expected limits. In Figure 6a, predictions are also shown for a topcolor Z′ model based on Refs. [4–6] updated to $\sqrt{s} = 7$ TeV in Ref. [57], with $\Gamma_{Z'}/m_{Z'} = 1.2\%$ and $\Gamma_{Z'}/m_{Z'} = 3\%$, compared to limits obtained assuming a 1% width. Higher-order QCD corrections to the Z′ production cross section were accounted for through a constant K-factor, computed to be 1.3. The same Z′ model, but for $\Gamma_{Z'}/m_{Z'} = 10\%$, is compared to the limits obtained assuming a 10% width in Fig. 6b. Finally, in Fig. 6c, the prediction of the Randall–Sundrum Kaluza–Klein gluon model from Ref. [12] is compared to the limits from data.

Using the upper limits for the Z′ with 1% width, mass ranges for two Z′ models are excluded as seen in Fig. 6a. First, the mass range 1.0–1.6 TeV/c^2 is excluded for a topcolor Z′ with width $\Gamma_{Z'}/m_{Z'} = 3\%$. Second, two mass ranges, 1.3–1.5 TeV/c^2 and a narrow range (smaller than the mass increment) close to 1.0 TeV/c^2, are excluded for the same topcolor Z′ with width $\Gamma_{Z'}/m_{Z'} = 1.2\%$. Similarly, using the upper limits for the Z′ with 10% width as seen in Fig. 6b, the mass range 1.0–2.0 TeV is excluded for a topcolor Z′ with width $\Gamma_{Z'}/m_{Z'} = 10\%$.

Finally, as seen in Fig. 6c, upper limits in the range of 1 pb are set on $\sigma_{g'} \times B(g' \to \mathrm{t\bar{t}})$ for $m_{g'} > 1.4$ TeV/c^2 for a specific Randall–Sundrum gluon model [12], which exclude the existence of this particle with masses between 1.4–1.5 TeV/c^2, as well as in a narrow region (smaller than the mass increment) close to 1.0 TeV/c^2.

The resonant analysis is cross-checked by counting events in specified mass windows of $m_{\mathrm{t\bar{t}}}$. The signal region is defined by a window in $m_{\mathrm{t\bar{t}}}$, and the background estimates from Figs. 5a and 5b are integrated over this range. The results obtained from this cross-check are consistent with the analysis of the $m_{\mathrm{t\bar{t}}}$ spectrum, but are not as sensitive. Table 2 shows the number

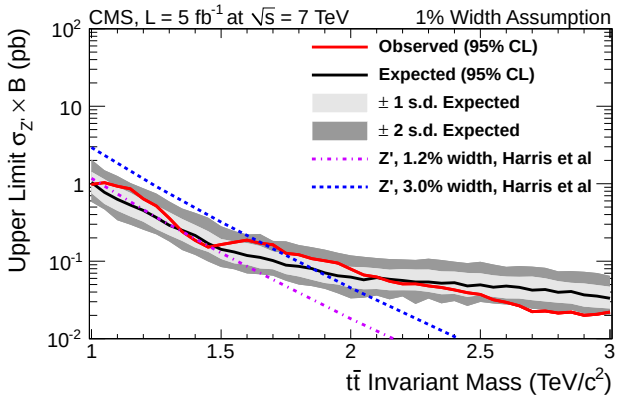

(a)

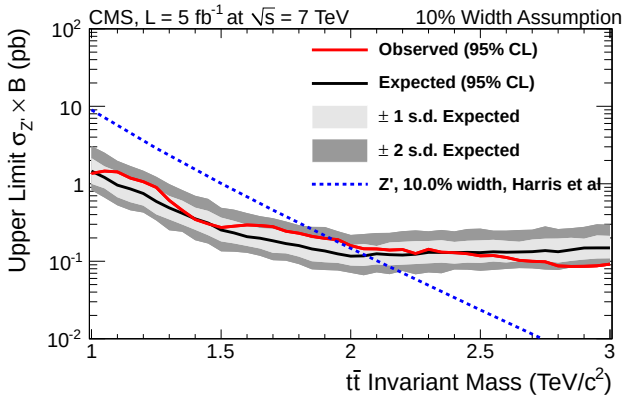

(b)

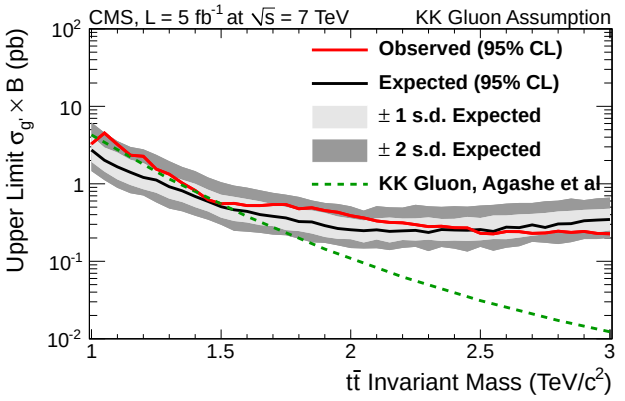

(c)

Figure 6: The 95% CL upper limits on the product of production cross section (σ) and branching fraction (B) of hypothesized objects into $t\bar{t}$, as a function of assumed resonance mass. (a) Z' production with $\Gamma_{Z'}/m_{Z'} = 1\%$ (1% width assumption) compared to predictions based on Refs. [4–6] for $\Gamma_{Z'}/m_{Z'}$ =1.2% and 3.0%. (b) Z' production with $\Gamma_{Z'}/m_{Z'} = 10\%$ (10% width assumption) compared to predictions based on Refs. [4–6] for a width of 10%. (c) Randall–Sundrum Kaluza–Klein gluon production from Ref. [12], compared to the theoretical prediction of that model. The ± 1 and ± 2 standard deviation (s.d.) excursions are shown relative to the results expected for the available luminosity.

Table 4: Expected number of events with $m_{t\bar{t}} > 1\,\text{TeV}/c^2$ from SM $t\bar{t}$ and non-top multijet backgrounds, along with their total, compared to the observed number of events. The efficiency for SM $t\bar{t}$ production, which is used in the limit setting procedure described in the text, is shown on the final line.

	1+1	1+2
Expected SM $t\bar{t}$ events	194 ± 106	129 ± 80
Expected non-top multijet events	1546 ± 45	2271 ± 130
Total expected events	1740 ± 115	2400 ± 153
Observed events	1738	2423
$t\bar{t}$ efficiency	$(2.5 \pm 1.3) \times 10^{-4}$	$(1.6 \pm 1.0) \times 10^{-4}$

of events observed and expected in two mass windows for the 1+1 and 1+2 channels, 0.9–1.1 TeV/c^2 corresponding to the $1\,\text{TeV}/c^2$ Z' sample, and 1.3–2.4 TeV/c^2 corresponding to the $2\,\text{TeV}/c^2$ Z' sample. The observed 95% CL upper limits on signal cross section change from 1.0 to 2.0 pb at $1\,\text{TeV}/c^2$, from 0.10 to 0.26 pb at $2\,\text{TeV}/c^2$, and from 0.02 to 0.05 pb at $3\,\text{TeV}/c^2$. Most of the difference is attributed to a better statistical handling in the resonance analysis of the bins with large background in the mass distribution.

5.2 $t\bar{t}$ enhancement analysis

In the second analysis, general enhancement is assumed in modeling the $t\bar{t}$ mass spectrum due to some new phenomenon (NP), assuming the same signal efficiency as for the SM $t\bar{t}$ continuum, as described in Refs. [22, 23]. The limit on any possible enhancement is presented in terms of a variable $\mathcal{S}$, the ratio of the integral of the $m_{t\bar{t}}$ distribution above $1\,\text{TeV}/c^2$ corresponding to SM $t\bar{t}$ production and a contribution from some NP, to that from just SM $t\bar{t}$ production:

$$\mathcal{S} = \frac{\int_{m_{t\bar{t}}>1\,\text{TeV}/c^2} \frac{d\sigma_{SM+NP}}{dm_{t\bar{t}}} dm_{t\bar{t}}}{\int_{m_{t\bar{t}}>1\,\text{TeV}/c^2} \frac{d\sigma_{SM}}{dm_{t\bar{t}}} dm_{t\bar{t}}}. \tag{4}$$

The events used for setting the limit are selected to have reconstructed $m_{t\bar{t}} > 1\,\text{TeV}/c^2$, which does not correspond to the same range for the true mass. Consequently, a correction factor must be applied to the reconstructed $t\bar{t}$ mass distribution to estimate the true mass distribution. This is estimated by dividing the number of simulated $t\bar{t}$ events with a reconstructed mass $> 1\,\text{TeV}/c^2$ by the number of simulated $t\bar{t}$ events with a true mass $> 1\,\text{TeV}/c^2$. This ratio is 1.24 $\pm$ 0.08 for the Type 1+1 analysis and 1.41 $\pm$ 0.11 for the Type 1+2 analysis. These differences are applied as multiplicative factors to obtain the yields for the true $t\bar{t}$ mass above $1\,\text{TeV}/c^2$. These factors do not affect the quantity $\mathcal{S}$ since they cancel in the ratio.

The approximate NNLO cross section for inclusive $t\bar{t}$ production is taken to be 163 pb [48–50]. The efficiency for Type 1+1 events, relative to inclusive SM $t\bar{t}$ production, is found to be $(2.5 \pm 1.3) \times 10^{-4}$, and for Type 1+2, the efficiency is $(1.6 \pm 1.0) \times 10^{-4}$. The numbers of observed and expected events for the SM $t\bar{t}$ and NTMJ backgrounds are shown in Table 4, along with these efficiencies. Following the statistical procedure outlined above, it follows that the enhancement factor to the $t\bar{t}$ production cross section for $m_{t\bar{t}} > 1\,\text{TeV}/c^2$ ($\mathcal{S}$ in Eq. (4)) must be < 2.6. The a priori expectation is for this limit to lie in the interval 2.0–3.5 at 68% CL, and 1.7–5.5 at 95% CL, with a most probable value of 2.5.

6 Summary

In summary, a search is presented for a massive resonance (Z') decaying into a $t\bar{t}$ pair in the all-hadronic final state using an integrated luminosity of $5\,fb^{-1}$ collected with the CMS detector at 7 TeV. A Z' with standard-model couplings is considered as a model of such a resonance. Two widths are considered ($\Gamma_{Z'}/m_{Z'} = 1\%$ and 10%), as well as an additional model of a Randall–Sundrum Kaluza–Klein gluon. The search focuses on high $t\bar{t}$ masses that yield collimated decay products, partially or fully merged into single jets. The analysis therefore relies on new developments in the area of jet substructure, thereby providing suppression of non-top multijet production.

No excess of events is observed over the expected yield from SM background sources. Upper limits in the range of 1 pb are set on the product of the Z' cross section and branching fraction for a topcolor Z' modeled for several widths, as well as for a Randall–Sundrum Kaluza–Klein gluon.

Finally, results are presented for any generic source of new phenomena with the same reconstruction efficiency as standard-model $t\bar{t}$ production, and limits are placed on any enhancement to the cross section from such a contribution. In particular, the $t\bar{t}$ production cross section (in total) must be less than a factor of 2.6 times that of the SM expectation for $m_{t\bar{t}} > 1\,\text{TeV}/c^2$. This constrains generic enhancements to standard-model $t\bar{t}$ production, which can be used to check models that seek to interpret the forward-backward $t\bar{t}$ production asymmetry observed at the Tevatron as a sign of new physics.

This is the first publication to constrain $t\bar{t}$ resonances in the kinematic region of $m_{t\bar{t}} > 1\,\text{TeV}/c^2$, and is also the first work to use the jet-substructure tools described above.

Acknowledgements

We thank Seung J. Lee for the computations of the Kaluza-Klein gluon cross sections at 7 TeV. We congratulate our colleagues in the CERN accelerator departments for the excellent performance of the LHC machine. We thank the technical and administrative staff at CERN and other CMS institutes, and acknowledge support from: FMSR (Austria); FNRS and FWO (Belgium); CNPq, CAPES, FAPERJ, and FAPESP (Brazil); MES (Bulgaria); CERN; CAS, MoST, and NSFC (China); COLCIENCIAS (Colombia); MSES (Croatia); RPF (Cyprus); MoER, SF0690030s09 and ERDF (Estonia); Academy of Finland, MEC, and HIP (Finland); CEA and CNRS/IN2P3 (France); BMBF, DFG, and HGF (Germany); GSRT (Greece); OTKA and NKTH (Hungary); DAE and DST (India); IPM (Iran); SFI (Ireland); INFN (Italy); NRF and WCU (Korea); LAS (Lithuania); CINVESTAV, CONACYT, SEP, and UASLP-FAI (Mexico); MSI (New Zealand); PAEC (Pakistan); MSHE and NSC (Poland); FCT (Portugal); JINR (Armenia, Belarus, Georgia, Ukraine, Uzbekistan); MON, RosAtom, RAS and RFBR (Russia); MSTD (Serbia); MICINN and CPAN (Spain); Swiss Funding Agencies (Switzerland); NSC (Taipei); TUBITAK and TAEK (Turkey); STFC (United Kingdom); DOE and NSF (USA).

This work was supported in part by the DOE under under Task TeV of contract DE-FG02-96ER40956 during the Workshop on Jet Substructure at the University of Washington.

References

[1] S. Dimopoulos and H. Georgi, "Softly Broken Supersymmetry and SU(5)", *Nucl. Phys. B* **193** (1981) 150–162, doi:10.1016/0550-3213(81)90522-8.

[2] S. Weinberg, "Implications of Dynamical Symmetry Breaking", *Phys. Rev. D* **13** (1976) 974–996, doi:10.1103/PhysRevD.13.974.

[3] L. Susskind, "Dynamics of Spontaneous Symmetry Breaking in the Weinberg- Salam Theory", *Phys. Rev. D* **20** (1979) 2619–2625, doi:10.1103/PhysRevD.20.2619.

[4] C. T. Hill and S. J. Parke, "Top production: Sensitivity to new physics", *Phys. Rev. D* **49** (1994) 4454–4462, doi:10.1103/PhysRevD.49.4454, arXiv:hep-ph/9312324.

[5] C. T. Hill, "Topcolor: Top quark condensation in a gauge extension of the standard model", *Phys. Lett. B* **266** (1991) 419–424, doi:10.1016/0370-2693(91)91061-Y. Updates in arXiv:hep-ph/9911288 and arXiv:hep-ph/1112.4928.

[6] C. T. Hill, "Topcolor assisted technicolor", *Phys. Lett. B* **345** (1995) 483–489, doi:10.1016/0370-2693(94)01660-5, arXiv:hep-ph/9411426.

[7] R. S. Chivukula et al., "Top quark seesaw theory of electroweak symmetry breaking", *Phys. Rev. D* **59** (1999) 075003, doi:10.1103/PhysRevD.59.075003, arXiv:hep-ph/9809470.

[8] N. Arkani-Hamed, A. G. Cohen, and H. Georgi, "Electroweak symmetry breaking from dimensional deconstruction", *Phys. Lett. B* **513** (2001) 232–240, doi:10.1016/S0370-2693(01)00741-9, arXiv:hep-ph/0105239.

[9] N. Arkani-Hamed, S. Dimopoulos, and G. R. Dvali, "The hierarchy problem and new dimensions at a millimeter", *Phys. Lett. B* **429** (1998) 263–272, doi:10.1016/S0370-2693(98)00466-3, arXiv:hep-ph/9803315.

[10] L. Randall and R. Sundrum, "A large mass hierarchy from a small extra dimension", *Phys. Rev. Lett.* **83** (1999) 3370–3373, doi:10.1103/PhysRevLett.83.3370, arXiv:hep-ph/9905221.

[11] L. Randall and R. Sundrum, "An alternative to compactification", *Phys. Rev. Lett.* **83** (1999) 4690–4693, doi:10.1103/PhysRevLett.83.4690, arXiv:hep-th/9906064.

[12] K. Agashe et al., "LHC signals from warped extra dimensions", *Phys. Rev. D* **77** (2008) 015003, doi:10.1103/PhysRevD.77.015003, arXiv:hep-ph/0612015.

[13] Y. Bai et al., "LHC Predictions from a Tevatron Anomaly in the Top Quark Forward-Backward Asymmetry", *JHEP* **03** (2011) 003, doi:10.1007/JHEP03(2011)003, arXiv:1101.5203.

[14] P. H. Frampton, J. Shu, and K. Wang, "Axigluon as Possible Explanation for $p\bar{p} \to t\bar{t}$ Forward-Backward Asymmetry", *Phys. Lett. B* **683** (2010) 294–297, doi:10.1016/j.physletb.2009.12.043, arXiv:0911.2955.

[15] M. I. Gresham, I.-W. Kim, and K. M. Zurek, "On Models of New Physics for the Tevatron Top A_FB", *Phys. Rev. D* **83** (2011) 114027, doi:10.1103/PhysRevD.83.114027, arXiv:1103.3501.

[16] O. Antunano, J. H. Kuhn, and G. Rodrigo, "Top quarks, axigluons and charge asymmetries at hadron colliders", *Phys. Rev. D* **77** (2008) 014003, doi:10.1103/PhysRevD.77.014003, arXiv:0709.1652.

[17] CDF Collaboration, "Forward-Backward Asymmetry in Top Quark Production in $p\bar{p}$ Collisions at $\sqrt{s}$ = 1.96 TeV", *Phys. Rev. Lett.* **101** (2008) 202001, doi:10.1103/PhysRevLett.101.202001, arXiv:0806.2472.

[18] D0 Collaboration, "First measurement of the forward-backward charge asymmetry in top quark pair production", *Phys. Rev. Lett.* **100** (2008) 142002, doi:10.1103/PhysRevLett.100.142002, arXiv:0712.0851.

[19] CDF Collaboration, "Evidence for a Mass Dependent Forward-Backward Asymmetry in Top Quark Pair Production", *Phys. Rev. D* **83** (2011) 112003, doi:10.1103/PhysRevD.83.112003, arXiv:1101.0034.

[20] D0 Collaboration, "Forward-backward asymmetry in top quark-antiquark production", *Phys. Rev. D* **84** (2011) 112005, doi:10.1103/PhysRevD.84.112005, arXiv:1107.4995.

[21] CDF Collaboration, "Evidence for a Mass Dependent Forward-Backward Asymmetry in Top Quark Pair Production", *Phys. Rev. D* **83** (2011) 112003, doi:10.1103/PhysRevD.83.112003, arXiv:1101.0034.

[22] C. Delaunay et al., "Implications of the CDF $t\bar{t}$ Forward-Backward Asymmetry for Hard Top Physics", *JHEP* **08** (2011) 031, doi:10.1007/JHEP08(2011)031, arXiv:1103.2297.

[23] J. A. Aguilar-Saavedra and M. Perez-Victoria, "Probing the Tevatron $t\bar{t}$ asymmetry at LHC", *JHEP* **05** (2011) 034, doi:10.1007/JHEP05(2011)034, arXiv:1103.2765.

[24] CDF Collaboration, "Limits on the production of narrow $t\bar{t}$ resonances in $p\bar{p}$ collisions at $\sqrt{s} = 1.96$ TeV", *Phys. Rev. D* **77** (2008) 051102, doi:10.1103/PhysRevD.77.051102, arXiv:0710.5335.

[25] CDF Collaboration, "Search for resonant $t\bar{t}$ production in $p\bar{p}$ collisions at $\sqrt{s}$ = 1.96 TeV", *Phys. Rev. Lett.* **100** (2008) 231801, doi:10.1103/PhysRevLett.100.231801, arXiv:0709.0705.

[26] D0 Collaboration, "Search for a Narrow $t\bar{t}$ Resonance in $p\bar{p}$ Collisions at $\sqrt{s} = 1.96$ TeV", *Phys. Rev. D* **85** (2012) 051101, doi:10.1103/PhysRevD.85.051101, arXiv:1111.1271.

[27] D. E. Kaplan et al., "Top Tagging: A Method for Identifying Boosted Hadronically Decaying Top Quarks", *Phys. Rev. Lett.* **101** (2008) 142001, doi:10.1103/PhysRevLett.101.142001, arXiv:0806.0848.

[28] CMS Collaboration, "A Cambridge-Aachen (C-A) based Jet Algorithm for boosted top-jet tagging", CMS Physics Analysis Summary CMS-PAS-JME-009-01, (2009).

[29] S. D. Ellis, C. K. Vermilion, and J. R. Walsh, "Techniques for improved heavy particle searches with jet substructure", *Phys. Rev. D* **80** (2009) 051501, doi:10.1103/PhysRevD.80.051501, arXiv:0903.5081.

[30] S. D. Ellis, C. K. Vermilion, and J. R. Walsh, "Recombination Algorithms and Jet Substructure: Pruning as a Tool for Heavy Particle Searches", *Phys. Rev. D* **81** (2010) 094023, doi:10.1103/PhysRevD.81.094023, arXiv:0912.0033.

[31] J. M. Butterworth et al., "Jet substructure as a new Higgs search channel at the LHC", *Phys. Rev. Lett.* **100** (2008) 242001, doi:10.1103/PhysRevLett.100.242001, arXiv:0802.2470.

[32] CMS Collaboration, "The CMS experiment at the CERN LHC", *JINST* **3** (2008) S08004, doi:10.1088/1748-0221/3/08/S08004.

[33] J. Alwall et al., "MadGraph/MadEvent v4: the new web generation", *JHEP* **09** (2007) 028, doi:10.1088/1126-6708/2007/09/028, arXiv:0706.2334.

[34] T. Sjöstrand et al., "High-energy physics event generation with PYTHIA 6.1", *Comput. Phys. Commun.* **135** (2001) 238–259, doi:10.1016/S0010-4655(00)00236-8, arXiv:hep-ph/0010017.

[35] T. Sjostrand, S. Mrenna, and P. Z. Skands, "A Brief Introduction to PYTHIA 8.1", *Comput. Phys. Commun.* **178** (2008) 852–867, doi:10.1016/j.cpc.2008.01.036, arXiv:0710.3820.

[36] J. Pumplin et al., "New generation of parton distributions with uncertainties from global QCD analysis", *JHEP* **07** (2002) 012, doi:10.1088/1126-6708/2002/07/012, arXiv:hep-ph/0201195.

[37] J. Allison et al., "Geant4 developments and applications", *IEEE Trans. Nucl. Sci.* **53** (2006) 270, doi:10.1109/TNS.2006.869826.

[38] CMS Collaboration, "Particle-Flow Event Reconstruction in CMS and Performance for Jets, Taus, and MET", CMS Physics Analysis Summary CMS-PAS-PFT-09-01, (2009).

[39] CMS Collaboration, "Tracking and Vertexing Results from First Collisions", CMS Physics Analysis Summary CMS-PAS-TRK-10-001, (2010).

[40] M. Wobisch and T. Wengler, "Hadronization corrections to jet cross sections in deep-inelastic scattering", *DESY-PROC* **02** (1998) arXiv:hep-ph/9907280.

[41] Y. L. Dokshitzer et al., "Better Jet Clustering Algorithms", *JHEP* **08** (1997) 001, doi:10.1088/1126-6708/1997/08/001, arXiv:hep-ph/9707323.

[42] M. Cacciari and G. P. Salam, "Dispelling the N**3 myth for the k(t) jet-finder", *Phys. Lett. B* **641** (2006) 57–61, doi:10.1016/j.physletb.2006.08.037, arXiv:hep-ph/0512210.

[43] M. Cacciari, G. P. Salam, and G. Soyez, "FastJet user manual", (2011). arXiv:1111.6097.

[44] M. Cacciari, G. P. Salam, and G. Soyez, "The anti-kt jet clustering algorithm", *JHEP* **04** (2008) 063, arXiv:0802.1189.

[45] CMS Collaboration, "Determination of Jet Energy Calibration and Transverse Momentum Resolution in CMS", *JINST* **6** (2011) P11002, doi:10.1088/1748-0221/6/11/P11002, arXiv:1107.4277.

[46] CMS Collaboration, "Measurement of the t $\bar{t}$ Production Cross Section in pp Collisions at 7 TeV in Lepton + Jets Events Using b-quark Jet Identification", *Phys. Rev. D* **84** (2011) 092004, doi:10.1103/PhysRevD.84.092004, arXiv:1108.3773.

[47] CMS Collaboration, "Performance of the b-jet identification in CMS", CMS Physics Analysis Summary CMS-PAS-BTV-11-001, (2011).

[48] M. Aliev et al., "HATHOR: HAdronic Top and Heavy quarks crOss section calculatoR", *Comput. Phys. Commun.* **182** (2011) 1034, doi:10.1016/j.cpc.2010.12.040, arXiv:1007.1327.

[49] U. Langenfeld, S. Moch, and P. Uwer, "Measuring the running top-quark mass", *Phys. Rev. D* **80** (2009) 054009, doi:10.1103/PhysRevD.80.054009, arXiv:0906.5273.

[50] N. Kidonakis, "Next-to-next-to-leading soft-gluon corrections for the top quark cross section and transverse momentum distribution", *Phys. Rev. D* **82** (2010) 114030, doi:10.1103/PhysRevD.82.114030, arXiv:1009.4935.

[51] K. Melnikov and F. Petriello, "Electroweak gauge boson production at hadron colliders through $O(\alpha_s^2)$", *Phys. Rev. D* **74** (2006) 114017, doi:10.1103/PhysRevD.74.114017, arXiv:hep-ph/0609070.

[52] S. D. Ellis et al., "Jets in hadron-hadron collisions", *Prog. Part. Nucl. Phys.* **60** (2008) 484–551, doi:10.1016/j.ppnp.2007.12.002, arXiv:0712.2447.

[53] G. Watt, "Parton distribution function dependence of benchmark Standard Model total cross sections at the 7 TeV LHC", *JHEP* **09** (2011) 069, doi:10.1007/JHEP09(2011)069, arXiv:1106.5788.

[54] A. L. Read, "Presentation of search results: the CLs technique", *J. Phys. G* **28** (2002) 2693, doi:10.1088/0954-3899/28/10/313.

[55] T. Junk, "Confidence level computation for combining searches with small statistics", *Nucl. Instrum. Meth. A* **434** (1999) 435, doi:10.1016/S0168-9002(99)00498-2.

[56] ATLAS and CMS Collaborations, "Procedure for the LHC Higgs boson search combination in summer 2011", ATL-PHYS-PUB-2011-011, CMS NOTE-11-005, (2011).

[57] R. M. Harris and S. Jain, "Cross Sections for Leptophobic Topcolor Z' decaying to top-antitop", *Eur. Phys. J. C* **72** (2012) 2072, arXiv:1112.4928.

A The CMS Collaboration

Yerevan Physics Institute, Yerevan, Armenia
S. Chatrchyan, V. Khachatryan, A.M. Sirunyan, A. Tumasyan

Institut für Hochenergiephysik der OeAW, Wien, Austria
W. Adam, T. Bergauer, M. Dragicevic, J. Erö, C. Fabjan, M. Friedl, R. Frühwirth, V.M. Ghete, J. Hammer[1], N. Hörmann, J. Hrubec, M. Jeitler, W. Kiesenhofer, M. Krammer, D. Liko, I. Mikulec, M. Pernicka[†], B. Rahbaran, C. Rohringer, H. Rohringer, R. Schöfbeck, J. Strauss, A. Taurok, F. Teischinger, P. Wagner, W. Waltenberger, G. Walzel, E. Widl, C.-E. Wulz

National Centre for Particle and High Energy Physics, Minsk, Belarus
V. Mossolov, N. Shumeiko, J. Suarez Gonzalez

Universiteit Antwerpen, Antwerpen, Belgium
S. Bansal, K. Cerny, T. Cornelis, E.A. De Wolf, X. Janssen, S. Luyckx, T. Maes, L. Mucibello, S. Ochesanu, B. Roland, R. Rougny, M. Selvaggi, H. Van Haevermaet, P. Van Mechelen, N. Van Remortel, A. Van Spilbeeck

Vrije Universiteit Brussel, Brussel, Belgium
F. Blekman, S. Blyweert, J. D'Hondt, R. Gonzalez Suarez, A. Kalogeropoulos, M. Maes, A. Olbrechts, W. Van Doninck, P. Van Mulders, G.P. Van Onsem, I. Villella

Université Libre de Bruxelles, Bruxelles, Belgium
O. Charaf, B. Clerbaux, G. De Lentdecker, V. Dero, A.P.R. Gay, T. Hreus, A. Léonard, P.E. Marage, T. Reis, L. Thomas, C. Vander Velde, P. Vanlaer

Ghent University, Ghent, Belgium
V. Adler, K. Beernaert, A. Cimmino, S. Costantini, G. Garcia, M. Grunewald, B. Klein, J. Lellouch, A. Marinov, J. Mccartin, A.A. Ocampo Rios, D. Ryckbosch, N. Strobbe, F. Thyssen, M. Tytgat, L. Vanelderen, P. Verwilligen, S. Walsh, E. Yazgan, N. Zaganidis

Université Catholique de Louvain, Louvain-la-Neuve, Belgium
S. Basegmez, G. Bruno, L. Ceard, C. Delaere, T. du Pree, D. Favart, L. Forthomme, A. Giammanco[2], J. Hollar, V. Lemaitre, J. Liao, O. Militaru, C. Nuttens, D. Pagano, A. Pin, K. Piotrzkowski, N. Schul

Université de Mons, Mons, Belgium
N. Beliy, T. Caebergs, E. Daubie, G.H. Hammad

Centro Brasileiro de Pesquisas Fisicas, Rio de Janeiro, Brazil
G.A. Alves, M. Correa Martins Junior, D. De Jesus Damiao, T. Martins, M.E. Pol, M.H.G. Souza

Universidade do Estado do Rio de Janeiro, Rio de Janeiro, Brazil
W.L. Aldá Júnior, W. Carvalho, A. Custódio, E.M. Da Costa, C. De Oliveira Martins, S. Fonseca De Souza, D. Matos Figueiredo, L. Mundim, H. Nogima, V. Oguri, W.L. Prado Da Silva, A. Santoro, S.M. Silva Do Amaral, L. Soares Jorge, A. Sznajder

Instituto de Fisica Teorica, Universidade Estadual Paulista, Sao Paulo, Brazil
T.S. Anjos[3], C.A. Bernardes[3], F.A. Dias[4], T.R. Fernandez Perez Tomei, E. M. Gregores[3], C. Lagana, F. Marinho, P.G. Mercadante[3], S.F. Novaes, Sandra S. Padula

Institute for Nuclear Research and Nuclear Energy, Sofia, Bulgaria
V. Genchev[1], P. Iaydjiev[1], S. Piperov, M. Rodozov, S. Stoykova, G. Sultanov, V. Tcholakov, R. Trayanov, M. Vutova

University of Sofia, Sofia, Bulgaria
A. Dimitrov, R. Hadjiiska, A. Karadzhinova, V. Kozhuharov, L. Litov, B. Pavlov, P. Petkov

Institute of High Energy Physics, Beijing, China
J.G. Bian, G.M. Chen, H.S. Chen, C.H. Jiang, D. Liang, S. Liang, X. Meng, J. Tao, J. Wang, J. Wang, X. Wang, Z. Wang, H. Xiao, M. Xu, J. Zang, Z. Zhang

State Key Lab. of Nucl. Phys. and Tech., Peking University, Beijing, China
C. Asawatangtrakuldee, Y. Ban, S. Guo, Y. Guo, W. Li, S. Liu, Y. Mao, S.J. Qian, H. Teng, S. Wang, B. Zhu, W. Zou

Universidad de Los Andes, Bogota, Colombia
C. Avila, B. Gomez Moreno, A.F. Osorio Oliveros, J.C. Sanabria

Technical University of Split, Split, Croatia
N. Godinovic, D. Lelas, R. Plestina[5], D. Polic, I. Puljak[1]

University of Split, Split, Croatia
Z. Antunovic, M. Dzelalija, M. Kovac

Institute Rudjer Boskovic, Zagreb, Croatia
V. Brigljevic, S. Duric, K. Kadija, J. Luetic, S. Morovic

University of Cyprus, Nicosia, Cyprus
A. Attikis, M. Galanti, G. Mavromanolakis, J. Mousa, C. Nicolaou, F. Ptochos, P.A. Razis

Charles University, Prague, Czech Republic
M. Finger, M. Finger Jr.

Academy of Scientific Research and Technology of the Arab Republic of Egypt, Egyptian Network of High Energy Physics, Cairo, Egypt
Y. Assran[6], S. Elgammal, A. Ellithi Kamel[7], S. Khalil[8], M.A. Mahmoud[9], A. Radi[8,10]

National Institute of Chemical Physics and Biophysics, Tallinn, Estonia
M. Kadastik, M. Müntel, M. Raidal, L. Rebane, A. Tiko

Department of Physics, University of Helsinki, Helsinki, Finland
V. Azzolini, P. Eerola, G. Fedi, M. Voutilainen

Helsinki Institute of Physics, Helsinki, Finland
S. Czellar, J. Härkönen, A. Heikkinen, V. Karimäki, R. Kinnunen, M.J. Kortelainen, T. Lampén, K. Lassila-Perini, S. Lehti, T. Lindén, P. Luukka, T. Mäenpää, T. Peltola, E. Tuominen, J. Tuominiemi, E. Tuovinen, D. Ungaro, L. Wendland

Lappeenranta University of Technology, Lappeenranta, Finland
K. Banzuzi, A. Korpela, T. Tuuva

Laboratoire d'Annecy-le-Vieux de Physique des Particules, IN2P3-CNRS, Annecy-le-Vieux, France
D. Sillou

DSM/IRFU, CEA/Saclay, Gif-sur-Yvette, France
M. Besancon, S. Choudhury, M. Dejardin, D. Denegri, B. Fabbro, J.L. Faure, F. Ferri, S. Ganjour, A. Givernaud, P. Gras, G. Hamel de Monchenault, P. Jarry, E. Locci, J. Malcles, L. Millischer, A. Nayak, J. Rander, A. Rosowsky, I. Shreyber, M. Titov

Laboratoire Leprince-Ringuet, Ecole Polytechnique, IN2P3-CNRS, Palaiseau, France
S. Baffioni, F. Beaudette, L. Benhabib, L. Bianchini, M. Bluj[11], C. Broutin, P. Busson, C. Charlot, N. Daci, T. Dahms, L. Dobrzynski, R. Granier de Cassagnac, M. Haguenauer, P. Miné, C. Mironov, C. Ochando, P. Paganini, D. Sabes, R. Salerno, Y. Sirois, C. Veelken, A. Zabi

Institut Pluridisciplinaire Hubert Curien, Université de Strasbourg, Université de Haute Alsace Mulhouse, CNRS/IN2P3, Strasbourg, France
J.-L. Agram[12], J. Andrea, D. Bloch, D. Bodin, J.-M. Brom, M. Cardaci, E.C. Chabert, C. Collard, E. Conte[12], F. Drouhin[12], C. Ferro, J.-C. Fontaine[12], D. Gelé, U. Goerlach, P. Juillot, M. Karim[12], A.-C. Le Bihan, P. Van Hove

Centre de Calcul de l'Institut National de Physique Nucleaire et de Physique des Particules (IN2P3), Villeurbanne, France
F. Fassi, D. Mercier

Université de Lyon, Université Claude Bernard Lyon 1, CNRS-IN2P3, Institut de Physique Nucléaire de Lyon, Villeurbanne, France
C. Baty, S. Beauceron, N. Beaupere, M. Bedjidian, O. Bondu, G. Boudoul, D. Boumediene, H. Brun, J. Chasserat, R. Chierici[1], D. Contardo, P. Depasse, H. El Mamouni, A. Falkiewicz, J. Fay, S. Gascon, M. Gouzevitch, B. Ille, T. Kurca, T. Le Grand, M. Lethuillier, L. Mirabito, S. Perries, V. Sordini, S. Tosi, Y. Tschudi, P. Verdier, S. Viret

Institute of High Energy Physics and Informatization, Tbilisi State University, Tbilisi, Georgia
Z. Tsamalaidze[13]

RWTH Aachen University, I. Physikalisches Institut, Aachen, Germany
G. Anagnostou, S. Beranek, M. Edelhoff, L. Feld, N. Heracleous, O. Hindrichs, R. Jussen, K. Klein, J. Merz, A. Ostapchuk, A. Perieanu, F. Raupach, J. Sammet, S. Schael, D. Sprenger, H. Weber, B. Wittmer, V. Zhukov[14]

RWTH Aachen University, III. Physikalisches Institut A, Aachen, Germany
M. Ata, J. Caudron, E. Dietz-Laursonn, D. Duchardt, M. Erdmann, A. Güth, T. Hebbeker, C. Heidemann, K. Hoepfner, T. Klimkovich, D. Klingebiel, P. Kreuzer, D. Lanske†, J. Lingemann, C. Magass, M. Merschmeyer, A. Meyer, M. Olschewski, P. Papacz, H. Pieta, H. Reithler, S.A. Schmitz, L. Sonnenschein, J. Steggemann, D. Teyssier, M. Weber

RWTH Aachen University, III. Physikalisches Institut B, Aachen, Germany
M. Bontenackels, V. Cherepanov, M. Davids, G. Flügge, H. Geenen, M. Geisler, W. Haj Ahmad, F. Hoehle, B. Kargoll, T. Kress, Y. Kuessel, A. Linn, A. Nowack, L. Perchalla, O. Pooth, J. Rennefeld, P. Sauerland, A. Stahl

Deutsches Elektronen-Synchrotron, Hamburg, Germany
M. Aldaya Martin, J. Behr, W. Behrenhoff, U. Behrens, M. Bergholz[15], A. Bethani, K. Borras, A. Burgmeier, A. Cakir, L. Calligaris, A. Campbell, E. Castro, F. Costanza, D. Dammann, G. Eckerlin, D. Eckstein, D. Fischer, G. Flucke, A. Geiser, I. Glushkov, S. Habib, J. Hauk, H. Jung[1], M. Kasemann, P. Katsas, C. Kleinwort, H. Kluge, A. Knutsson, M. Krämer, D. Krücker, E. Kuznetsova, W. Lange, W. Lohmann[15], B. Lutz, R. Mankel, I. Marfin, M. Marienfeld, I.-A. Melzer-Pellmann, A.B. Meyer, J. Mnich, A. Mussgiller, S. Naumann-Emme, J. Olzem, H. Perrey, A. Petrukhin, D. Pitzl, A. Raspereza, P.M. Ribeiro Cipriano, C. Riedl, M. Rosin, J. Salfeld-Nebgen, R. Schmidt[15], T. Schoerner-Sadenius, N. Sen, A. Spiridonov, M. Stein, R. Walsh, C. Wissing

University of Hamburg, Hamburg, Germany
C. Autermann, V. Blobel, S. Bobrovskyi, J. Draeger, H. Enderle, J. Erfle, U. Gebbert, M. Görner, T. Hermanns, R.S. Höing, K. Kaschube, G. Kaussen, H. Kirschenmann, R. Klanner, J. Lange, B. Mura, F. Nowak, N. Pietsch, D. Rathjens, C. Sander, H. Schettler, P. Schleper, E. Schlieckau, A. Schmidt, M. Schröder, T. Schum, M. Seidel, H. Stadie, G. Steinbrück, J. Thomsen

Institut für Experimentelle Kernphysik, Karlsruhe, Germany
C. Barth, J. Berger, T. Chwalek, W. De Boer, A. Dierlamm, M. Feindt, M. Guthoff[1], C. Hackstein, F. Hartmann, M. Heinrich, H. Held, K.H. Hoffmann, S. Honc, U. Husemann, I. Katkov[14], J.R. Komaragiri, D. Martschei, S. Mueller, Th. Müller, M. Niegel, A. Nürnberg, O. Oberst, A. Oehler, J. Ott, T. Peiffer, G. Quast, K. Rabbertz, F. Ratnikov, N. Ratnikova, S. Röcker, C. Saout, A. Scheurer, F.-P. Schilling, M. Schmanau, G. Schott, H.J. Simonis, F.M. Stober, D. Troendle, R. Ulrich, J. Wagner-Kuhr, T. Weiler, M. Zeise, E.B. Ziebarth

Institute of Nuclear Physics "Demokritos", Aghia Paraskevi, Greece
G. Daskalakis, T. Geralis, S. Kesisoglou, A. Kyriakis, D. Loukas, I. Manolakos, A. Markou, C. Markou, C. Mavrommatis, E. Ntomari

University of Athens, Athens, Greece
L. Gouskos, T.J. Mertzimekis, A. Panagiotou, N. Saoulidou

University of Ioánnina, Ioánnina, Greece
I. Evangelou, C. Foudas[1], P. Kokkas, N. Manthos, I. Papadopoulos, V. Patras

KFKI Research Institute for Particle and Nuclear Physics, Budapest, Hungary
G. Bencze, C. Hajdu[1], P. Hidas, D. Horvath[16], A. Kapusi, K. Krajczar[17], B. Radics, F. Sikler[1], V. Veszpremi, G. Vesztergombi[17]

Institute of Nuclear Research ATOMKI, Debrecen, Hungary
N. Beni, J. Molnar, J. Palinkas, Z. Szillasi

University of Debrecen, Debrecen, Hungary
J. Karancsi, P. Raics, Z.L. Trocsanyi, B. Ujvari

Panjab University, Chandigarh, India
S.B. Beri, V. Bhatnagar, N. Dhingra, R. Gupta, M. Jindal, M. Kaur, J.M. Kohli, M.Z. Mehta, N. Nishu, L.K. Saini, A. Sharma, J. Singh, S.P. Singh

University of Delhi, Delhi, India
S. Ahuja, B.C. Choudhary, A. Kumar, A. Kumar, S. Malhotra, M. Naimuddin, K. Ranjan, V. Sharma, R.K. Shivpuri

Saha Institute of Nuclear Physics, Kolkata, India
S. Banerjee, S. Bhattacharya, S. Dutta, B. Gomber, Sa. Jain, Sh. Jain, R. Khurana, S. Sarkar

Bhabha Atomic Research Centre, Mumbai, India
A. Abdulsalam, R.K. Choudhury, D. Dutta, S. Kailas, V. Kumar, A.K. Mohanty[1], L.M. Pant, P. Shukla

Tata Institute of Fundamental Research - EHEP, Mumbai, India
T. Aziz, S. Ganguly, M. Guchait[18], A. Gurtu[19], M. Maity[20], G. Majumder, K. Mazumdar, G.B. Mohanty, B. Parida, K. Sudhakar, N. Wickramage

Tata Institute of Fundamental Research - HECR, Mumbai, India
S. Banerjee, S. Dugad

Institute for Research in Fundamental Sciences (IPM), Tehran, Iran
H. Arfaei, H. Bakhshiansohi[21], S.M. Etesami[22], A. Fahim[21], M. Hashemi, H. Hesari, A. Jafari[21], M. Khakzad, A. Mohammadi[23], M. Mohammadi Najafabadi, S. Paktinat Mehdiabadi, B. Safarzadeh[24], M. Zeinali[22]

INFN Sezione di Bari [a], Università di Bari [b], Politecnico di Bari [c], Bari, Italy
M. Abbrescia[a,b], L. Barbone[a,b], C. Calabria[a,b,1], S.S. Chhibra[a,b], A. Colaleo[a], D. Creanza[a,c], N. De Filippis[a,c,1], M. De Palma[a,b], L. Fiore[a], G. Iaselli[a,c], L. Lusito[a,b], G. Maggi[a,c], M. Maggi[a], B. Marangelli[a,b], S. My[a,c], S. Nuzzo[a,b], N. Pacifico[a,b], A. Pompili[a,b], G. Pugliese[a,c], G. Selvaggi[a,b], L. Silvestris[a], G. Singh[a,b], G. Zito[a]

INFN Sezione di Bologna [a], Università di Bologna [b], Bologna, Italy
G. Abbiendi[a], A.C. Benvenuti[a], D. Bonacorsi[a,b], S. Braibant-Giacomelli[a,b], L. Brigliadori[a,b], P. Capiluppi[a,b], A. Castro[a,b], F.R. Cavallo[a], M. Cuffiani[a,b], G.M. Dallavalle[a], F. Fabbri[a], A. Fanfani[a,b], D. Fasanella[a,b,1], P. Giacomelli[a], C. Grandi[a], L. Guiducci, S. Marcellini[a], G. Masetti[a], M. Meneghelli[a,b,1], A. Montanari[a], F.L. Navarria[a,b], F. Odorici[a], A. Perrotta[a], F. Primavera[a,b], A.M. Rossi[a,b], T. Rovelli[a,b], G. Siroli[a,b], R. Travaglini[a,b]

INFN Sezione di Catania [a], Università di Catania [b], Catania, Italy
S. Albergo[a,b], G. Cappello[a,b], M. Chiorboli[a,b], S. Costa[a,b], R. Potenza[a,b], A. Tricomi[a,b], C. Tuve[a,b]

INFN Sezione di Firenze [a], Università di Firenze [b], Firenze, Italy
G. Barbagli[a], V. Ciulli[a,b], C. Civinini[a], R. D'Alessandro[a,b], E. Focardi[a,b], S. Frosali[a,b], E. Gallo[a], S. Gonzi[a,b], M. Meschini[a], S. Paoletti[a], G. Sguazzoni[a], A. Tropiano[a,1]

INFN Laboratori Nazionali di Frascati, Frascati, Italy
L. Benussi, S. Bianco, S. Colafranceschi[25], F. Fabbri, D. Piccolo

INFN Sezione di Genova, Genova, Italy
P. Fabbricatore, R. Musenich

INFN Sezione di Milano-Bicocca [a], Università di Milano-Bicocca [b], Milano, Italy
A. Benaglia[a,b,1], F. De Guio[a,b], L. Di Matteo[a,b,1], S. Fiorendi[a,b], S. Gennai[a,1], A. Ghezzi[a,b], S. Malvezzi[a], R.A. Manzoni[a,b], A. Martelli[a,b], A. Massironi[a,b,1], D. Menasce[a], L. Moroni[a], M. Paganoni[a,b], D. Pedrini[a], S. Ragazzi[a,b], N. Redaelli[a], S. Sala[a], T. Tabarelli de Fatis[a,b]

INFN Sezione di Napoli [a], Università di Napoli "Federico II" [b], Napoli, Italy
S. Buontempo[a], C.A. Carrillo Montoya[a,1], N. Cavallo[a,26], A. De Cosa[a,b], O. Dogangun[a,b], F. Fabozzi[a,26], A.O.M. Iorio[a,1], L. Lista[a], S. Meola[a,27], M. Merola[a,b], P. Paolucci[a]

INFN Sezione di Padova [a], Università di Padova [b], Università di Trento (Trento) [c], Padova, Italy
P. Azzi[a], N. Bacchetta[a,1], P. Bellan[a,b], D. Bisello[a,b], A. Branca[a,1], R. Carlin[a,b], P. Checchia[a], T. Dorigo[a], U. Dosselli[a], F. Gasparini[a,b], A. Gozzelino[a], K. Kanishchev[a,c], S. Lacaprara[a,28], I. Lazzizzera[a,c], M. Margoni[a,b], A.T. Meneguzzo[a,b], M. Nespolo[a,1], L. Perrozzi[a], N. Pozzobon[a,b], P. Ronchese[a,b], F. Simonetto[a,b], E. Torassa[a], M. Tosi[a,b,1], S. Vanini[a,b], P. Zotto[a,b]

INFN Sezione di Pavia [a], Università di Pavia [b], Pavia, Italy
M. Gabusi[a,b], S.P. Ratti[a,b], C. Riccardi[a,b], P. Torre[a,b], P. Vitulo[a,b]

INFN Sezione di Perugia [a], Università di Perugia [b], Perugia, Italy
G.M. Bilei[a], L. Fanò[a,b], P. Lariccia[a,b], A. Lucaroni[a,b,1], G. Mantovani[a,b], M. Menichelli[a], A. Nappi[a,b], F. Romeo[a,b], A. Saha, A. Santocchia[a,b], S. Taroni[a,b,1]

INFN Sezione di Pisa [a], Università di Pisa [b], Scuola Normale Superiore di Pisa [c], Pisa, Italy
P. Azzurri[a,c], G. Bagliesi[a], T. Boccali[a], G. Broccolo[a,c], R. Castaldi[a], R.T. D'Agnolo[a,c], R. Dell'Orso[a], F. Fiori[a,b], L. Foà[a,c], A. Giassi[a], A. Kraan[a], F. Ligabue[a,c], T. Lomtadze[a], L. Martini[a,29], A. Messineo[a,b], F. Palla[a], F. Palmonari[a], A. Rizzi[a,b], A.T. Serban[a,30], P. Spagnolo[a], R. Tenchini[a], G. Tonelli[a,b,1], A. Venturi[a,1], P.G. Verdini[a]

INFN Sezione di Roma [a], Università di Roma "La Sapienza" [b], Roma, Italy
L. Barone[a,b], F. Cavallari[a], D. Del Re[a,b,1], M. Diemoz[a], C. Fanelli[a,b], M. Grassi[a,1], E. Longo[a,b], P. Meridiani[a,1], F. Micheli[a,b], S. Nourbakhsh[a], G. Organtini[a,b], F. Pandolfi[a,b], R. Paramatti[a], S. Rahatlou[a,b], M. Sigamani[a], L. Soffi[a,b]

INFN Sezione di Torino [a], Università di Torino [b], Università del Piemonte Orientale (Novara) [c], Torino, Italy
N. Amapane[a,b], R. Arcidiacono[a,c], S. Argiro[a,b], M. Arneodo[a,c], C. Biino[a], C. Botta[a,b], N. Cartiglia[a], R. Castello[a,b], M. Costa[a,b], N. Demaria[a], A. Graziano[a,b], C. Mariotti[a,1], S. Maselli[a], G. Mazza, E. Migliore[a,b], V. Monaco[a,b], M. Musich[a,1], M.M. Obertino[a,c], N. Pastrone[a], M. Pelliccioni[a], A. Potenza[a,b], A. Romero[a,b], M. Ruspa[a,c], R. Sacchi[a,b], A. Solano[a,b], A. Staiano[a], A. Vilela Pereira[a]

INFN Sezione di Trieste [a], Università di Trieste [b], Trieste, Italy
S. Belforte[a], F. Cossutti[a], G. Della Ricca[a,b], B. Gobbo[a], M. Marone[a,b,1], D. Montanino[a,b,1], A. Penzo[a], A. Schizzi[a,b]

Kangwon National University, Chunchon, Korea
S.G. Heo, T.Y. Kim, S.K. Nam

Kyungpook National University, Daegu, Korea
S. Chang, J. Chung, D.H. Kim, G.N. Kim, D.J. Kong, H. Park, S.R. Ro, D.C. Son

Chonnam National University, Institute for Universe and Elementary Particles, Kwangju, Korea
J.Y. Kim, Zero J. Kim, S. Song

Konkuk University, Seoul, Korea
H.Y. Jo

Korea University, Seoul, Korea
S. Choi, D. Gyun, B. Hong, M. Jo, H. Kim, T.J. Kim, K.S. Lee, D.H. Moon, S.K. Park, E. Seo

University of Seoul, Seoul, Korea
M. Choi, S. Kang, H. Kim, J.H. Kim, C. Park, I.C. Park, S. Park, G. Ryu

Sungkyunkwan University, Suwon, Korea
Y. Cho, Y. Choi, Y.K. Choi, J. Goh, M.S. Kim, B. Lee, J. Lee, S. Lee, H. Seo, I. Yu

Vilnius University, Vilnius, Lithuania
M.J. Bilinskas, I. Grigelionis, M. Janulis, A. Juodagalvis

Centro de Investigacion y de Estudios Avanzados del IPN, Mexico City, Mexico
H. Castilla-Valdez, E. De La Cruz-Burelo, I. Heredia-de La Cruz, R. Lopez-Fernandez, R. Magaña Villalba, J. Martínez-Ortega, A. Sánchez-Hernández, L.M. Villasenor-Cendejas

Universidad Iberoamericana, Mexico City, Mexico
S. Carrillo Moreno, F. Vazquez Valencia

Benemerita Universidad Autonoma de Puebla, Puebla, Mexico
H.A. Salazar Ibarguen

Universidad Autónoma de San Luis Potosí, San Luis Potosí, Mexico
E. Casimiro Linares, A. Morelos Pineda, M.A. Reyes-Santos

University of Auckland, Auckland, New Zealand
D. Krofcheck

University of Canterbury, Christchurch, New Zealand
A.J. Bell, P.H. Butler, R. Doesburg, S. Reucroft, H. Silverwood

National Centre for Physics, Quaid-I-Azam University, Islamabad, Pakistan
M. Ahmad, M.I. Asghar, H.R. Hoorani, S. Khalid, W.A. Khan, T. Khurshid, S. Qazi, M.A. Shah, M. Shoaib

Institute of Experimental Physics, Faculty of Physics, University of Warsaw, Warsaw, Poland
G. Brona, M. Cwiok, W. Dominik, K. Doroba, A. Kalinowski, M. Konecki, J. Krolikowski

Soltan Institute for Nuclear Studies, Warsaw, Poland
H. Bialkowska, B. Boimska, T. Frueboes, R. Gokieli, M. Górski, M. Kazana, K. Nawrocki, K. Romanowska-Rybinska, M. Szleper, G. Wrochna, P. Zalewski

Laboratório de Instrumentação e Física Experimental de Partículas, Lisboa, Portugal
N. Almeida, P. Bargassa, A. David, P. Faccioli, P.G. Ferreira Parracho, M. Gallinaro, P. Musella, J. Pela[1], J. Seixas, J. Varela, P. Vischia

Joint Institute for Nuclear Research, Dubna, Russia
I. Belotelov, P. Bunin, M. Gavrilenko, I. Golutvin, V. Karjavin, V. Konoplyanikov, G. Kozlov, A. Lanev, A. Malakhov, P. Moisenz, V. Palichik, V. Perelygin, M. Savina, S. Shmatov, V. Smirnov, A. Volodko, A. Zarubin

Petersburg Nuclear Physics Institute, Gatchina (St Petersburg), Russia
S. Evstyukhin, V. Golovtsov, Y. Ivanov, V. Kim, P. Levchenko, V. Murzin, V. Oreshkin, I. Smirnov, V. Sulimov, L. Uvarov, S. Vavilov, A. Vorobyev, An. Vorobyev

Institute for Nuclear Research, Moscow, Russia
Yu. Andreev, A. Dermenev, S. Gninenko, N. Golubev, M. Kirsanov, N. Krasnikov, V. Matveev, A. Pashenkov, D. Tlisov, A. Toropin

Institute for Theoretical and Experimental Physics, Moscow, Russia
V. Epshteyn, M. Erofeeva, V. Gavrilov, M. Kossov[1], N. Lychkovskaya, V. Popov, G. Safronov, S. Semenov, V. Stolin, E. Vlasov, A. Zhokin

Moscow State University, Moscow, Russia
A. Belyaev, E. Boos, M. Dubinin[4], L. Dudko, A. Ershov, A. Gribushin, V. Klyukhin, O. Kodolova, I. Lokhtin, A. Markina, S. Obraztsov, M. Perfilov, S. Petrushanko, L. Sarycheva[†], V. Savrin, A. Snigirev

P.N. Lebedev Physical Institute, Moscow, Russia
V. Andreev, M. Azarkin, I. Dremin, M. Kirakosyan, A. Leonidov, G. Mesyats, S.V. Rusakov, A. Vinogradov

State Research Center of Russian Federation, Institute for High Energy Physics, Protvino, Russia
I. Azhgirey, I. Bayshev, S. Bitioukov, V. Grishin[1], V. Kachanov, D. Konstantinov, A. Korablev,

V. Krychkine, V. Petrov, R. Ryutin, A. Sobol, L. Tourtchanovitch, S. Troshin, N. Tyurin, A. Uzunian, A. Volkov

University of Belgrade, Faculty of Physics and Vinca Institute of Nuclear Sciences, Belgrade, Serbia
P. Adzic[31], M. Djordjevic, M. Ekmedzic, D. Krpic[31], J. Milosevic

Centro de Investigaciones Energéticas Medioambientales y Tecnológicas (CIEMAT), Madrid, Spain
M. Aguilar-Benitez, J. Alcaraz Maestre, P. Arce, C. Battilana, E. Calvo, M. Cerrada, M. Chamizo Llatas, N. Colino, B. De La Cruz, A. Delgado Peris, C. Diez Pardos, D. Domínguez Vázquez, C. Fernandez Bedoya, J.P. Fernández Ramos, A. Ferrando, J. Flix, M.C. Fouz, P. Garcia-Abia, O. Gonzalez Lopez, S. Goy Lopez, J.M. Hernandez, M.I. Josa, G. Merino, J. Puerta Pelayo, I. Redondo, L. Romero, J. Santaolalla, M.S. Soares, C. Willmott

Universidad Autónoma de Madrid, Madrid, Spain
C. Albajar, G. Codispoti, J.F. de Trocóniz

Universidad de Oviedo, Oviedo, Spain
J. Cuevas, J. Fernandez Menendez, S. Folgueras, I. Gonzalez Caballero, L. Lloret Iglesias, J. Piedra Gomez[32], J.M. Vizan Garcia

Instituto de Física de Cantabria (IFCA), CSIC-Universidad de Cantabria, Santander, Spain
J.A. Brochero Cifuentes, I.J. Cabrillo, A. Calderon, S.H. Chuang, J. Duarte Campderros, M. Felcini[33], M. Fernandez, G. Gomez, J. Gonzalez Sanchez, C. Jorda, P. Lobelle Pardo, A. Lopez Virto, J. Marco, R. Marco, C. Martinez Rivero, F. Matorras, F.J. Munoz Sanchez, T. Rodrigo, A.Y. Rodríguez-Marrero, A. Ruiz-Jimeno, L. Scodellaro, M. Sobron Sanudo, I. Vila, R. Vilar Cortabitarte

CERN, European Organization for Nuclear Research, Geneva, Switzerland
D. Abbaneo, E. Auffray, G. Auzinger, P. Baillon, A.H. Ball, D. Barney, C. Bernet[5], G. Bianchi, P. Bloch, A. Bocci, A. Bonato, H. Breuker, K. Bunkowski, T. Camporesi, G. Cerminara, T. Christiansen, J.A. Coarasa Perez, D. D'Enterria, A. De Roeck, S. Di Guida, M. Dobson, N. Dupont-Sagorin, A. Elliott-Peisert, B. Frisch, W. Funk, G. Georgiou, M. Giffels, D. Gigi, K. Gill, D. Giordano, M. Giunta, F. Glege, R. Gomez-Reino Garrido, P. Govoni, S. Gowdy, R. Guida, M. Hansen, P. Harris, C. Hartl, J. Harvey, B. Hegner, A. Hinzmann, V. Innocente, P. Janot, K. Kaadze, E. Karavakis, K. Kousouris, P. Lecoq, P. Lenzi, C. Lourenço, T. Mäki, M. Malberti, L. Malgeri, M. Mannelli, L. Masetti, F. Meijers, S. Mersi, E. Meschi, R. Moser, M.U. Mozer, M. Mulders, E. Nesvold, M. Nguyen, T. Orimoto, L. Orsini, E. Palencia Cortezon, E. Perez, A. Petrilli, A. Pfeiffer, M. Pierini, M. Pimiä, D. Piparo, G. Polese, L. Quertenmont, A. Racz, W. Reece, J. Rodrigues Antunes, G. Rolandi[34], T. Rommerskirchen, C. Rovelli[35], M. Rovere, H. Sakulin, F. Santanastasio, C. Schäfer, C. Schwick, I. Segoni, S. Sekmen, A. Sharma, P. Siegrist, P. Silva, M. Simon, P. Sphicas[36], D. Spiga, M. Spiropulu[4], M. Stoye, A. Tsirou, G.I. Veres[17], J.R. Vlimant, H.K. Wöhri, S.D. Worm[37], W.D. Zeuner

Paul Scherrer Institut, Villigen, Switzerland
W. Bertl, K. Deiters, W. Erdmann, K. Gabathuler, R. Horisberger, Q. Ingram, H.C. Kaestli, S. König, D. Kotlinski, U. Langenegger, F. Meier, D. Renker, T. Rohe, J. Sibille[38]

Institute for Particle Physics, ETH Zurich, Zurich, Switzerland
L. Bäni, P. Bortignon, M.A. Buchmann, B. Casal, N. Chanon, Z. Chen, A. Deisher, G. Dissertori, M. Dittmar, M. Dünser, J. Eugster, K. Freudenreich, C. Grab, P. Lecomte, W. Lustermann,

A.C. Marini, P. Martinez Ruiz del Arbol, N. Mohr, F. Moortgat, C. Nägeli[39], P. Nef, F. Nessi-Tedaldi, L. Pape, F. Pauss, M. Peruzzi, F.J. Ronga, M. Rossini, L. Sala, A.K. Sanchez, A. Starodumov[40], B. Stieger, M. Takahashi, L. Tauscher†, A. Thea, K. Theofilatos, D. Treille, C. Urscheler, R. Wallny, H.A. Weber, L. Wehrli

Universität Zürich, Zurich, Switzerland
E. Aguilo, C. Amsler, V. Chiochia, S. De Visscher, C. Favaro, M. Ivova Rikova, B. Millan Mejias, P. Otiougova, P. Robmann, H. Snoek, S. Tupputi, M. Verzetti

National Central University, Chung-Li, Taiwan
Y.H. Chang, K.H. Chen, A. Go, C.M. Kuo, S.W. Li, W. Lin, Z.K. Liu, Y.J. Lu, D. Mekterovic, A.P. Singh, R. Volpe, S.S. Yu

National Taiwan University (NTU), Taipei, Taiwan
P. Bartalini, P. Chang, Y.H. Chang, Y.W. Chang, Y. Chao, K.F. Chen, C. Dietz, U. Grundler, W.-S. Hou, Y. Hsiung, K.Y. Kao, Y.J. Lei, R.-S. Lu, D. Majumder, E. Petrakou, X. Shi, J.G. Shiu, Y.M. Tzeng, M. Wang

Cukurova University, Adana, Turkey
A. Adiguzel, M.N. Bakirci[41], S. Cerci[42], C. Dozen, I. Dumanoglu, E. Eskut, S. Girgis, G. Gokbulut, I. Hos, E.E. Kangal, G. Karapinar, A. Kayis Topaksu, G. Onengut, K. Ozdemir, S. Ozturk[43], A. Polatoz, K. Sogut[44], D. Sunar Cerci[42], B. Tali[42], H. Topakli[41], L.N. Vergili, M. Vergili

Middle East Technical University, Physics Department, Ankara, Turkey
I.V. Akin, T. Aliev, B. Bilin, S. Bilmis, M. Deniz, H. Gamsizkan, A.M. Guler, K. Ocalan, A. Ozpineci, M. Serin, R. Sever, U.E. Surat, M. Yalvac, E. Yildirim, M. Zeyrek

Bogazici University, Istanbul, Turkey
M. Deliomeroglu, E. Gülmez, B. Isildak, M. Kaya[45], O. Kaya[45], S. Ozkorucuklu[46], N. Sonmez[47]

Istanbul Technical University, Istanbul, Turkey
K. Cankocak

National Scientific Center, Kharkov Institute of Physics and Technology, Kharkov, Ukraine
L. Levchuk

University of Bristol, Bristol, United Kingdom
F. Bostock, J.J. Brooke, E. Clement, D. Cussans, H. Flacher, R. Frazier, J. Goldstein, M. Grimes, G.P. Heath, H.F. Heath, L. Kreczko, S. Metson, D.M. Newbold[37], K. Nirunpong, A. Poll, S. Senkin, V.J. Smith, T. Williams

Rutherford Appleton Laboratory, Didcot, United Kingdom
L. Basso[48], K.W. Bell, A. Belyaev[48], C. Brew, R.M. Brown, D.J.A. Cockerill, J.A. Coughlan, K. Harder, S. Harper, J. Jackson, B.W. Kennedy, E. Olaiya, D. Petyt, B.C. Radburn-Smith, C.H. Shepherd-Themistocleous, I.R. Tomalin, W.J. Womersley

Imperial College, London, United Kingdom
R. Bainbridge, G. Ball, R. Beuselinck, O. Buchmuller, D. Colling, N. Cripps, M. Cutajar, P. Dauncey, G. Davies, M. Della Negra, W. Ferguson, J. Fulcher, D. Futyan, A. Gilbert, A. Guneratne Bryer, G. Hall, Z. Hatherell, J. Hays, G. Iles, M. Jarvis, G. Karapostoli, L. Lyons, A.-M. Magnan, J. Marrouche, B. Mathias, R. Nandi, J. Nash, A. Nikitenko[40], A. Papageorgiou, M. Pesaresi, K. Petridis, M. Pioppi[49], D.M. Raymond, S. Rogerson, N. Rompotis, A. Rose, M.J. Ryan, C. Seez, P. Sharp†, A. Sparrow, A. Tapper, M. Vazquez Acosta, T. Virdee, S. Wakefield, N. Wardle, T. Whyntie

Brunel University, Uxbridge, United Kingdom
M. Barrett, M. Chadwick, J.E. Cole, P.R. Hobson, A. Khan, P. Kyberd, D. Leggat, D. Leslie, W. Martin, I.D. Reid, P. Symonds, L. Teodorescu, M. Turner

Baylor University, Waco, USA
K. Hatakeyama, H. Liu, T. Scarborough

The University of Alabama, Tuscaloosa, USA
C. Henderson, P. Rumerio

Boston University, Boston, USA
A. Avetisyan, T. Bose, C. Fantasia, A. Heister, J. St. John, P. Lawson, D. Lazic, J. Rohlf, D. Sperka, L. Sulak

Brown University, Providence, USA
J. Alimena, S. Bhattacharya, D. Cutts, A. Ferapontov, U. Heintz, S. Jabeen, G. Kukartsev, G. Landsberg, M. Luk, M. Narain, D. Nguyen, M. Segala, T. Sinthuprasith, T. Speer, K.V. Tsang

University of California, Davis, Davis, USA
R. Breedon, G. Breto, M. Calderon De La Barca Sanchez, S. Chauhan, M. Chertok, J. Conway, R. Conway, P.T. Cox, J. Dolen, R. Erbacher, M. Gardner, R. Houtz, W. Ko, A. Kopecky, R. Lander, O. Mall, T. Miceli, R. Nelson, D. Pellett, B. Rutherford, M. Searle, J. Smith, M. Squires, M. Tripathi, R. Vasquez Sierra

University of California, Los Angeles, Los Angeles, USA
V. Andreev, D. Cline, R. Cousins, J. Duris, S. Erhan, P. Everaerts, C. Farrell, J. Hauser, M. Ignatenko, C. Plager, G. Rakness, P. Schlein†, J. Tucker, V. Valuev, M. Weber

University of California, Riverside, Riverside, USA
J. Babb, R. Clare, M.E. Dinardo, J. Ellison, J.W. Gary, F. Giordano, G. Hanson, G.Y. Jeng[50], H. Liu, O.R. Long, A. Luthra, H. Nguyen, S. Paramesvaran, J. Sturdy, S. Sumowidagdo, R. Wilken, S. Wimpenny

University of California, San Diego, La Jolla, USA
W. Andrews, J.G. Branson, G.B. Cerati, S. Cittolin, D. Evans, F. Golf, A. Holzner, R. Kelley, M. Lebourgeois, J. Letts, I. Macneill, B. Mangano, J. Muelmenstaedt, S. Padhi, C. Palmer, G. Petrucciani, M. Pieri, R. Ranieri, M. Sani, V. Sharma, S. Simon, E. Sudano, M. Tadel, Y. Tu, A. Vartak, S. Wasserbaech[51], F. Würthwein, A. Yagil, J. Yoo

University of California, Santa Barbara, Santa Barbara, USA
D. Barge, R. Bellan, C. Campagnari, M. D'Alfonso, T. Danielson, K. Flowers, P. Geffert, J. Incandela, C. Justus, P. Kalavase, S.A. Koay, D. Kovalskyi[1], V. Krutelyov, S. Lowette, N. Mccoll, V. Pavlunin, F. Rebassoo, J. Ribnik, J. Richman, R. Rossin, D. Stuart, W. To, C. West

California Institute of Technology, Pasadena, USA
A. Apresyan, A. Bornheim, Y. Chen, E. Di Marco, J. Duarte, M. Gataullin, Y. Ma, A. Mott, H.B. Newman, C. Rogan, V. Timciuc, P. Traczyk, J. Veverka, R. Wilkinson, Y. Yang, R.Y. Zhu

Carnegie Mellon University, Pittsburgh, USA
B. Akgun, R. Carroll, T. Ferguson, Y. Iiyama, D.W. Jang, Y.F. Liu, M. Paulini, H. Vogel, I. Vorobiev

University of Colorado at Boulder, Boulder, USA
J.P. Cumalat, B.R. Drell, C.J. Edelmaier, W.T. Ford, A. Gaz, B. Heyburn, E. Luiggi Lopez, J.G. Smith, K. Stenson, K.A. Ulmer, S.R. Wagner

Cornell University, Ithaca, USA
L. Agostino, J. Alexander, A. Chatterjee, N. Eggert, L.K. Gibbons, B. Heltsley, W. Hopkins, A. Khukhunaishvili, B. Kreis, N. Mirman, G. Nicolas Kaufman, J.R. Patterson, A. Ryd, E. Salvati, W. Sun, W.D. Teo, J. Thom, J. Thompson, J. Vaughan, Y. Weng, L. Winstrom, P. Wittich

Fairfield University, Fairfield, USA
D. Winn

Fermi National Accelerator Laboratory, Batavia, USA
S. Abdullin, M. Albrow, J. Anderson, L.A.T. Bauerdick, A. Beretvas, J. Berryhill, P.C. Bhat, I. Bloch, K. Burkett, J.N. Butler, V. Chetluru, H.W.K. Cheung, F. Chlebana, V.D. Elvira, I. Fisk, J. Freeman, Y. Gao, D. Green, O. Gutsche, A. Hahn, J. Hanlon, R.M. Harris, J. Hirschauer, B. Hooberman, S. Jindariani, M. Johnson, U. Joshi, B. Kilminster, B. Klima, S. Kunori, S. Kwan, D. Lincoln, R. Lipton, L. Lueking, J. Lykken, K. Maeshima, J.M. Marraffino, S. Maruyama, D. Mason, P. McBride, K. Mishra, S. Mrenna, Y. Musienko[52], C. Newman-Holmes, V. O'Dell, O. Prokofyev, E. Sexton-Kennedy, S. Sharma, W.J. Spalding, L. Spiegel, P. Tan, L. Taylor, S. Tkaczyk, N.V. Tran, L. Uplegger, E.W. Vaandering, R. Vidal, J. Whitmore, W. Wu, F. Yang, F. Yumiceva, J.C. Yun

University of Florida, Gainesville, USA
D. Acosta, P. Avery, D. Bourilkov, M. Chen, S. Das, M. De Gruttola, G.P. Di Giovanni, D. Dobur, A. Drozdetskiy, R.D. Field, M. Fisher, Y. Fu, I.K. Furic, J. Gartner, J. Hugon, B. Kim, J. Konigsberg, A. Korytov, A. Kropivnitskaya, T. Kypreos, J.F. Low, K. Matchev, P. Milenovic[53], G. Mitselmakher, L. Muniz, R. Remington, A. Rinkevicius, P. Sellers, N. Skhirtladze, M. Snowball, J. Yelton, M. Zakaria

Florida International University, Miami, USA
V. Gaultney, L.M. Lebolo, S. Linn, P. Markowitz, G. Martinez, J.L. Rodriguez

Florida State University, Tallahassee, USA
T. Adams, A. Askew, J. Bochenek, J. Chen, B. Diamond, S.V. Gleyzer, J. Haas, S. Hagopian, V. Hagopian, M. Jenkins, K.F. Johnson, H. Prosper, V. Veeraraghavan, M. Weinberg

Florida Institute of Technology, Melbourne, USA
M.M. Baarmand, B. Dorney, M. Hohlmann, H. Kalakhety, I. Vodopiyanov

University of Illinois at Chicago (UIC), Chicago, USA
M.R. Adams, I.M. Anghel, L. Apanasevich, Y. Bai, V.E. Bazterra, R.R. Betts, J. Callner, R. Cavanaugh, C. Dragoiu, O. Evdokimov, E.J. Garcia-Solis, L. Gauthier, C.E. Gerber, D.J. Hofman, S. Khalatyan, F. Lacroix, M. Malek, C. O'Brien, C. Silkworth, D. Strom, N. Varelas

The University of Iowa, Iowa City, USA
U. Akgun, E.A. Albayrak, B. Bilki[54], K. Chung, W. Clarida, F. Duru, S. Griffiths, C.K. Lae, J.-P. Merlo, H. Mermerkaya[55], A. Mestvirishvili, A. Moeller, J. Nachtman, C.R. Newsom, E. Norbeck, J. Olson, Y. Onel, F. Ozok, S. Sen, E. Tiras, J. Wetzel, T. Yetkin, K. Yi

Johns Hopkins University, Baltimore, USA
B.A. Barnett, B. Blumenfeld, S. Bolognesi, D. Fehling, G. Giurgiu, A.V. Gritsan, Z.J. Guo, G. Hu, P. Maksimovic, S. Rappoccio, M. Swartz, A. Whitbeck

The University of Kansas, Lawrence, USA
P. Baringer, A. Bean, G. Benelli, O. Grachov, R.P. Kenny Iii, M. Murray, D. Noonan, V. Radicci, S. Sanders, R. Stringer, G. Tinti, J.S. Wood, V. Zhukova

Kansas State University, Manhattan, USA
A.F. Barfuss, T. Bolton, I. Chakaberia, A. Ivanov, S. Khalil, M. Makouski, Y. Maravin, S. Shrestha, I. Svintradze

Lawrence Livermore National Laboratory, Livermore, USA
J. Gronberg, D. Lange, D. Wright

University of Maryland, College Park, USA
A. Baden, M. Boutemeur, B. Calvert, S.C. Eno, J.A. Gomez, N.J. Hadley, R.G. Kellogg, M. Kirn, T. Kolberg, Y. Lu, M. Marionneau, A.C. Mignerey, A. Peterman, K. Rossato, A. Skuja, J. Temple, M.B. Tonjes, S.C. Tonwar, E. Twedt

Massachusetts Institute of Technology, Cambridge, USA
G. Bauer, J. Bendavid, W. Busza, E. Butz, I.A. Cali, M. Chan, V. Dutta, G. Gomez Ceballos, M. Goncharov, K.A. Hahn, Y. Kim, M. Klute, Y.-J. Lee, W. Li, P.D. Luckey, T. Ma, S. Nahn, C. Paus, D. Ralph, C. Roland, G. Roland, M. Rudolph, G.S.F. Stephans, F. Stöckli, K. Sumorok, K. Sung, D. Velicanu, E.A. Wenger, R. Wolf, B. Wyslouch, S. Xie, M. Yang, Y. Yilmaz, A.S. Yoon, M. Zanetti

University of Minnesota, Minneapolis, USA
S.I. Cooper, P. Cushman, B. Dahmes, A. De Benedetti, G. Franzoni, A. Gude, J. Haupt, S.C. Kao, K. Klapoetke, Y. Kubota, J. Mans, N. Pastika, V. Rekovic, R. Rusack, M. Sasseville, A. Singovsky, N. Tambe, J. Turkewitz

University of Mississippi, University, USA
L.M. Cremaldi, R. Kroeger, L. Perera, R. Rahmat, D.A. Sanders

University of Nebraska-Lincoln, Lincoln, USA
E. Avdeeva, K. Bloom, S. Bose, J. Butt, D.R. Claes, A. Dominguez, M. Eads, P. Jindal, J. Keller, I. Kravchenko, J. Lazo-Flores, H. Malbouisson, S. Malik, G.R. Snow

State University of New York at Buffalo, Buffalo, USA
U. Baur, A. Godshalk, I. Iashvili, S. Jain, A. Kharchilava, A. Kumar, S.P. Shipkowski, K. Smith

Northeastern University, Boston, USA
G. Alverson, E. Barberis, D. Baumgartel, M. Chasco, J. Haley, D. Trocino, D. Wood, J. Zhang

Northwestern University, Evanston, USA
A. Anastassov, A. Kubik, N. Mucia, N. Odell, R.A. Ofierzynski, B. Pollack, A. Pozdnyakov, M. Schmitt, S. Stoynev, M. Velasco, S. Won

University of Notre Dame, Notre Dame, USA
L. Antonelli, D. Berry, A. Brinkerhoff, M. Hildreth, C. Jessop, D.J. Karmgard, J. Kolb, K. Lannon, W. Luo, S. Lynch, N. Marinelli, D.M. Morse, T. Pearson, R. Ruchti, J. Slaunwhite, N. Valls, J. Warchol, M. Wayne, M. Wolf, J. Ziegler

The Ohio State University, Columbus, USA
B. Bylsma, L.S. Durkin, C. Hill, R. Hughes, P. Killewald, K. Kotov, T.Y. Ling, D. Puigh, M. Rodenburg, C. Vuosalo, G. Williams, B.L. Winer

Princeton University, Princeton, USA
N. Adam, E. Berry, P. Elmer, D. Gerbaudo, V. Halyo, P. Hebda, J. Hegeman, A. Hunt, E. Laird, D. Lopes Pegna, P. Lujan, D. Marlow, T. Medvedeva, M. Mooney, J. Olsen, P. Piroué, X. Quan, A. Raval, H. Saka, D. Stickland, C. Tully, J.S. Werner, A. Zuranski

University of Puerto Rico, Mayaguez, USA
J.G. Acosta, X.T. Huang, A. Lopez, H. Mendez, S. Oliveros, J.E. Ramirez Vargas, A. Zatserklyaniy

Purdue University, West Lafayette, USA
E. Alagoz, V.E. Barnes, D. Benedetti, G. Bolla, D. Bortoletto, M. De Mattia, A. Everett, Z. Hu, M. Jones, O. Koybasi, M. Kress, A.T. Laasanen, N. Leonardo, V. Maroussov, P. Merkel, D.H. Miller, N. Neumeister, I. Shipsey, D. Silvers, A. Svyatkovskiy, M. Vidal Marono, H.D. Yoo, J. Zablocki, Y. Zheng

Purdue University Calumet, Hammond, USA
S. Guragain, N. Parashar

Rice University, Houston, USA
A. Adair, C. Boulahouache, V. Cuplov, K.M. Ecklund, F.J.M. Geurts, B.P. Padley, R. Redjimi, J. Roberts, J. Zabel

University of Rochester, Rochester, USA
B. Betchart, A. Bodek, Y.S. Chung, R. Covarelli, P. de Barbaro, R. Demina, Y. Eshaq, A. Garcia-Bellido, P. Goldenzweig, Y. Gotra, J. Han, A. Harel, S. Korjenevski, D.C. Miner, D. Vishnevskiy, M. Zielinski

The Rockefeller University, New York, USA
A. Bhatti, R. Ciesielski, L. Demortier, K. Goulianos, G. Lungu, S. Malik, C. Mesropian

Rutgers, the State University of New Jersey, Piscataway, USA
S. Arora, A. Barker, J.P. Chou, C. Contreras-Campana, E. Contreras-Campana, D. Duggan, D. Ferencek, Y. Gershtein, R. Gray, E. Halkiadakis, D. Hidas, D. Hits, A. Lath, S. Panwalkar, M. Park, R. Patel, A. Richards, J. Robles, K. Rose, S. Salur, S. Schnetzer, C. Seitz, S. Somalwar, R. Stone, S. Thomas

University of Tennessee, Knoxville, USA
G. Cerizza, M. Hollingsworth, S. Spanier, Z.C. Yang, A. York

Texas A&M University, College Station, USA
R. Eusebi, W. Flanagan, J. Gilmore, T. Kamon[56], V. Khotilovich, R. Montalvo, I. Osipenkov, Y. Pakhotin, A. Perloff, J. Roe, A. Safonov, T. Sakuma, S. Sengupta, I. Suarez, A. Tatarinov, D. Toback

Texas Tech University, Lubbock, USA
N. Akchurin, J. Damgov, P.R. Dudero, C. Jeong, K. Kovitanggoon, S.W. Lee, T. Libeiro, Y. Roh, I. Volobouev

Vanderbilt University, Nashville, USA
E. Appelt, D. Engh, C. Florez, S. Greene, A. Gurrola, W. Johns, P. Kurt, C. Maguire, A. Melo, P. Sheldon, B. Snook, S. Tuo, J. Velkovska

University of Virginia, Charlottesville, USA
M.W. Arenton, M. Balazs, S. Boutle, B. Cox, B. Francis, J. Goodell, R. Hirosky, A. Ledovskoy, C. Lin, C. Neu, J. Wood, R. Yohay

Wayne State University, Detroit, USA
S. Gollapinni, R. Harr, P.E. Karchin, C. Kottachchi Kankanamge Don, P. Lamichhane, A. Sakharov

University of Wisconsin, Madison, USA
M. Anderson, M. Bachtis, D. Belknap, L. Borrello, D. Carlsmith, M. Cepeda, S. Dasu, L. Gray, K.S. Grogg, M. Grothe, R. Hall-Wilton, M. Herndon, A. Hervé, P. Klabbers, J. Klukas, A. Lanaro, C. Lazaridis, J. Leonard, R. Loveless, A. Mohapatra, I. Ojalvo, G.A. Pierro, I. Ross, A. Savin, W.H. Smith, J. Swanson

†: Deceased
1: Also at CERN, European Organization for Nuclear Research, Geneva, Switzerland
2: Also at National Institute of Chemical Physics and Biophysics, Tallinn, Estonia
3: Also at Universidade Federal do ABC, Santo Andre, Brazil
4: Also at California Institute of Technology, Pasadena, USA
5: Also at Laboratoire Leprince-Ringuet, Ecole Polytechnique, IN2P3-CNRS, Palaiseau, France
6: Also at Suez Canal University, Suez, Egypt
7: Also at Cairo University, Cairo, Egypt
8: Also at British University, Cairo, Egypt
9: Also at Fayoum University, El-Fayoum, Egypt
10: Now at Ain Shams University, Cairo, Egypt
11: Also at Soltan Institute for Nuclear Studies, Warsaw, Poland
12: Also at Université de Haute-Alsace, Mulhouse, France
13: Now at Joint Institute for Nuclear Research, Dubna, Russia
14: Also at Moscow State University, Moscow, Russia
15: Also at Brandenburg University of Technology, Cottbus, Germany
16: Also at Institute of Nuclear Research ATOMKI, Debrecen, Hungary
17: Also at Eötvös Loránd University, Budapest, Hungary
18: Also at Tata Institute of Fundamental Research - HECR, Mumbai, India
19: Now at King Abdulaziz University, Jeddah, Saudi Arabia
20: Also at University of Visva-Bharati, Santiniketan, India
21: Also at Sharif University of Technology, Tehran, Iran
22: Also at Isfahan University of Technology, Isfahan, Iran
23: Also at Shiraz University, Shiraz, Iran
24: Also at Plasma Physics Research Center, Science and Research Branch, Islamic Azad University, Teheran, Iran
25: Also at Facoltà Ingegneria Università di Roma, Roma, Italy
26: Also at Università della Basilicata, Potenza, Italy
27: Also at Università degli Studi Guglielmo Marconi, Roma, Italy
28: Also at Laboratori Nazionali di Legnaro dell' INFN, Legnaro, Italy
29: Also at Università degli studi di Siena, Siena, Italy
30: Also at University of Bucharest, Bucuresti-Magurele, Romania
31: Also at Faculty of Physics of University of Belgrade, Belgrade, Serbia
32: Also at University of Florida, Gainesville, USA
33: Also at University of California, Los Angeles, Los Angeles, USA
34: Also at Scuola Normale e Sezione dell' INFN, Pisa, Italy
35: Also at INFN Sezione di Roma; Università di Roma "La Sapienza", Roma, Italy
36: Also at University of Athens, Athens, Greece
37: Also at Rutherford Appleton Laboratory, Didcot, United Kingdom
38: Also at The University of Kansas, Lawrence, USA
39: Also at Paul Scherrer Institut, Villigen, Switzerland
40: Also at Institute for Theoretical and Experimental Physics, Moscow, Russia
41: Also at Gaziosmanpasa University, Tokat, Turkey
42: Also at Adiyaman University, Adiyaman, Turkey

43: Also at The University of Iowa, Iowa City, USA
44: Also at Mersin University, Mersin, Turkey
45: Also at Kafkas University, Kars, Turkey
46: Also at Suleyman Demirel University, Isparta, Turkey
47: Also at Ege University, Izmir, Turkey
48: Also at School of Physics and Astronomy, University of Southampton, Southampton, United Kingdom
49: Also at INFN Sezione di Perugia; Università di Perugia, Perugia, Italy
50: Also at University of Sydney, Sydney, Australia
51: Also at Utah Valley University, Orem, USA
52: Also at Institute for Nuclear Research, Moscow, Russia
53: Also at University of Belgrade, Faculty of Physics and Vinca Institute of Nuclear Sciences, Belgrade, Serbia
54: Also at Argonne National Laboratory, Argonne, USA
55: Also at Erzincan University, Erzincan, Turkey
56: Also at Kyungpook National University, Daegu, Korea